Pathogenic *de novo* variants in *PPP2R5C* cause a neurodevelopmental disorder within the Houge-Janssens syndrome spectrum

Authors

Iris Verbinnen, Sofia Douzgou Houge, Tzung-Chien Hsieh, ..., Peter Krawitz, Gunnar Douzgos Houge, Veerle Janssens

Correspondence

gunnar.douzgos.houge@helse-bergen.no (G.D.H.), veerle.janssens@kuleuven.be (V.J.)

By international gene matching, data mining from individuals with ultra-rare disorders, and biochemical studies, we identified pathogenic missense variants in *PPP2R5C* as a cause of a neurodevelopmental disorder within the Houge-Janssens syndrome spectrum. *PPP2R5C* encodes a protein phosphatase 2A (PP2A) substrate-binding subunit called B56γ. Disease-causing *PPP2R5C* variants have a dominant-negative effect.

Verbinnen et al., 2025, The American Journal of Human Genetics *112*, 1–18
March 6, 2025

https://doi.org/10.1016/j.ajhg.2025.01.021

CellPress

Please cite this article in press as: Verbinnen et al., Pathogenic *de novo* variants in *PPP2R5C* cause a neurodevelopmental disorder within the Houge-Janssens syndrome spectrum, The American Journal of Human Genetics (2025), https://doi.org/10.1016/j.ajhg.2025.01.021

ARTICLE

Pathogenic *de novo* variants in *PPP2R5C* cause a neurodevelopmental disorder within the Houge-Janssens syndrome spectrum

Iris Verbinnen,[1,2,71] Sofia Douzgou Houge,[3,4,71] Tzung-Chien Hsieh,[5] Hellen Lesmann,[6] Aron Kirchhoff,[5] David Geneviève,[7] Elise Brimble,[8] Lisa Lenaerts,[1] Dorien Haesen,[1] Rebecca J. Levy,[9] Julien Thevenon,[10] Laurence Faivre,[11,12] Elysa Marco,[13] Jessica X. Chong,[14] Mike Bamshad,[14,15] Karynne Patterson,[15] Ghayda M. Mirzaa,[14,16] Kimberly Foss,[17] William Dobyns,[18] Susan M. White,[19,20] Lynn Pais,[21] Emily O'Heir,[21,22] Raphaela Itzikowitz,[23] Kirsten A. Donald,[23] Celia Van der Merwe,[24,25] Alessandro Mussa,[26] Raffaela Cervini,[27] Elisa Giorgio,[28,29] Tony Roscioli,[30,31,32] Kerith-Rae Dias,[30,33] Carey-Anne Evans,[30,32] Natasha J. Brown,[34,35] Anna Ruiz,[36]

(Author list continued on next page)

Summary

Pathogenic variants resulting in protein phosphatase 2A (PP2A) dysfunction result in mild to severe neurodevelopmental delay. PP2A is a trimer of a catalytic (C) subunit, scaffolding (A) subunit, and substrate binding/regulatory (B) subunit, encoded by 19 different genes. *De novo* missense variants in *PPP2R5D* (B56δ) or *PPP2R1A* (Aα) and *de novo* missense and loss-of-function variants in *PPP2CA* (Cα) lead to syndromes with overlapping phenotypic features, known as Houge-Janssens syndrome (HJS) types 1, 2, and 3, respectively. Here, we describe an additional condition in the HJS spectrum in 26 individuals with variants in *PPP2R5C*, encoding the regulatory B56γ subunit. Most changes were *de novo* and of the missense type. The clinical features were well within the HJS spectrum with strongest resemblance to HJS type 1, caused by B56δ variants. Common features were neurodevelopmental delay and hypotonia, with a high risk of epilepsy, behavioral problems, and mildly dysmorphic facial features. Head circumferences were above average or macrocephalic. The degree of intellectual disability was, on average, milder than in other HJS types. All variants affected either substrate binding (2/19), C-subunit binding (2/19), or both (15/19). Five variants were recurrent. Catalytic activity of the phosphatase was variably affected by the variants. Of note, *PPP2R5C* total loss-of-function variants could be inherited from a non-symptomatic parent. This implies that a dominant-negative mechanism on substrate dephosphorylation or general PP2A function is the most likely pathogenic mechanism.

Introduction

Protein phosphatase 2A (PP2A)-related neurodevelopmental disorders, recently renamed as Houge-Janssens syndrome (HJS) (HJS1 [MIM: 616355], HJS2 [MIM: 616362], and HJS3 [MIM: 618354]), are a growing spectrum of genetic disorders, caused by heterozygous, *de novo*, pathogenic variants in *PPP2R5D* ([MIM: 601646], encoding the PP2A B56δ subunit, HJS1), *PPP2R1A* ([MIM: 605983], encoding the PP2A Aα subunit, HJS2), or *PPP2CA* ([MIM: 176915] encoding the PP2A Cα subunit, HJS3).[1–4] PP2A genes encode one of three subunits constituting the

[1]Laboratory of Protein Phosphorylation and Proteomics, KU Leuven Department of Cellular and Molecular Medicine, University of Leuven, Leuven, Belgium; [2]KU Leuven Institute for Rare Diseases (Leuven.IRD), Leuven, Belgium; [3]Department of Medical Genetics, Haukeland University Hospital, Bergen, Norway; [4]Department of Clinical Science, University of Bergen, Bergen, Norway; [5]Institute for Genomic Statistics and Bioinformatics, University Hospital Bonn, Rheinische Friedrich-Wilhelms-Universität Bonn, Bonn, Germany; [6]Institute of Human Genetics, University Hospital Bonn, Rheinische Friedrich-Wilhelms-Universität Bonn, Bonn, Germany; [7]Montpellier University, INSERM U1183, Centre de Référence Anomalies du développement et syndromes malformatifs, ERN ITHACA, Génétique clinique, CHU Montpellier, Montpellier, France; [8]Invitae, San Francisco, CA, USA; [9]Department of Neurology and Neurological Sciences, Stanford Medicine, Stanford, CA, USA; [10]CNRS UMR 5309, INSERM U1209, Institute of Advanced Biosciences, Université Grenoble-Alpes, Service Génomique et Procréation, Centre Hospitalo-Universitaire Grenoble Alpes, Cedex Grenoble, France; [11]Centre de génétique et Centre de Référence Anomalies du Développement et Syndromes Malformatifs, FHU TRANSLAD, Hôpital d'enfants, CHU Dijon Bourgogne, Dijon, France; [12]UMR1231 GAD, Inserm - Université Bourgogne-Franche Comté, Dijon, France; [13]Cortica Healthcare, San Rafael, CA, USA; [14]Division of Genetic Medicine, Department of Pediatrics, University of Washington School of Medicine, Seattle, WA, USA; [15]Department of Genome Sciences, University of Washington, Seattle, WA, USA; [16]Department of Laboratory Medicine and Pathology, University of Washington, Seattle, WA, USA; [17]Department of Genetics, University of North Carolina at Chapel Hill, Chapel Hill, NC, USA; [18]Department of Pediatrics, Division of Genetics and Metabolism, University of Minnesota, Minneapolis, MN, USA; [19]Victorian Clinical Genetics Services (VCGS), Royal Children's Hospital, Parkville, VIC, Australia; [20]Department of Paediatrics, University of Melbourne, Melbourne, VIC, Australia; [21]Center for Mendelian Genomics, Broad Institute of MIT and Harvard, Cambridge, MA, USA; [22]Division of Genetics and Genomics, Department of Pediatrics, Boston Children's Hospital, Boston, MA, USA; [23]Department of Paediatrics and Child Health, Red Cross War Memorial Children's Hospital, and the Neuroscience Institute, University of Cape Town, Cape Town, South Africa; [24]Stanley Center for Psychiatric Research, The Broad Institute, Cambridge, MA, USA; [25]Analytic and Translational Genetics Unit, Massachusetts General Hospital, Boston, MA, USA; [26]Department of Public Health and Pediatric Sciences, University of Torino, Regina Margherita Children's Hospital, Torino, Italy; [27]Child Neuropsychiatry Department, Maria Vittoria Hospital, Torino, Italy; [28]Department of Molecular Medicine, University of Pavia, Pavia, Italy; [29]IRCCS Mondino Foundation, Neurogenetics Research Centre, Pavia, Italy; [30]Neuroscience Research Australia (NeuRA), Sydney, NSW, Australia; [31]Centre for Clinical

(Affiliations continued on next page)

Please cite this article in press as: Verbinnen et al., Pathogenic *de novo* variants in *PPP2R5C* cause a neurodevelopmental disorder within the Houge-Janssens syndrome spectrum, The American Journal of Human Genetics (2025), https://doi.org/10.1016/j.ajhg.2025.01.021

Juan Pablo Trujillo Quintero,[37] Rachel Rabin,[38] John Pappas,[38] Hai Yuan,[39] Katherine Lachlan,[40] Simon Thomas,[41,42] Anita Devlin,[43,44] Michael Wright,[45] Richard Martin,[46] Joanna Karwowska,[47] Renata Posmyk,[47] Nicolas Chatron,[48,49] Zornitza Stark,[34,50,51] Oliver Heath,[34] Martin Delatycki,[34,51,52] Rebecca Buchert,[53] Georg-Christoph Korenke,[54] Keri Ramsey,[55] Vinodh Narayanan,[55] Dorothy K. Grange,[56] Judith L. Weisenberg,[57] Tobias B. Haack,[53,58] Stephanie Karch,[59] Patricia Kipkemoi,[60] Moses Mangi,[60] Karen G.C.B. Bindels de Heus,[61,62] Marie-Claire Y. de Wit,[62,63] Tahsin Stefan Barakat,[62,64,65] Derek Lim,[66] Géraldine Van Winckel,[67] Rebecca C. Spillmann,[68] Vandana Shashi,[68] Maureen Jacob,[69] Antonia M. Stehr,[69] The Undiagnosed Diseases Network,[70] Peter Krawitz,[5] Gunnar Douzgos Houge,[3,*] and Veerle Janssens[1,2,*]

functional PP2A enzymatic complexes, with the C subunit harboring the catalytic phosphatase activity, a regulatory B-type subunit conferring substrate specificity and regulation, and the structural A subunit scaffolding the C- and B-type subunits.[4–6] *PPP2CA*-related syndrome (HJS3) is characterized by variable neurodevelopmental features such as mild to profound intellectual disability, autism (50%), seizures (50%), brain abnormalities (micro- or macrocephaly and corpus callosum hypoplasia), and mild or no facial dysmorphism.[3,7,8] *PPP2R1A*-related syndrome (HJS2) is characterized by at least two distinctive clinical and biochemical subgroups.[1,9–12] Common features are hypotonia and developmental delay. The least severely affected *PPP2R1A* subgroup is characterized by intellectual disability with relative macrocephaly, absence of seizures, and, in some cases, microtia or hearing loss. The more severely affected subgroup presents with moderate to severe intellectual disability, microcephaly, seizures, corpus callosum hypoplasia/agenesis, and, less frequently, congenital heart defects.[1,9–12] Hypotonia, mild to severe intellectual disability, relative macrocephaly, and seizures are the most notable characteristics of the *PPP2R5D*-related syndrome (HJS1),[1,13–15] which also confers a risk for early-onset parkinsonism.[16–18]

Functional characterization of HJS variants revealed functional changes in almost all individuals, either by haploinsufficiency of the remaining wild-type (WT) allele (only proven for *PPP2CA*) or by dominant-negative effects of the variants.[1,3,9,15] However, despite increased mammalian target of rapamycin (mTOR) signaling and ribosomal S6 protein phosphorylation in HEK293 cells expressing the PPP2R5D Glu420Lys or Glu198Lys variant as a heterozygous knockin,[19,20] or increased AKT/mTOR signaling in HEC-1A cells overexpressing the PPP2R1A Arg183Gln variant,[21] the functional implications of most PP2A alterations on (neuronal) signaling and brain function remain largely unknown.

In 2015, a single case report described an overgrowth phenotype in association with a *de novo* variant (Thr126del) in another PP2A gene, *PPP2R5C* (MIM: 601645), encoding the regulatory B56γ subunit.[2] However, because of lack of functional characterization of the variant, a causal relationship between occurrence of the variant and the overgrowth phenotype has remained

Genetics, Sydney Children's Hospital, Sydney, NSW, Australia; [32]New South Wales Health Pathology Randwick Genomics, Prince of Wales Hospital, Sydney, NSW 2031, Australia; [33]Prince of Wales Clinical School, Faculty of Medicine, University of New South Wales, Sydney, NSW 2031, Australia; [34]Victorian Clinical Genetics Services, Murdoch Children's Research Institute, University of Melbourne, Parkville, VIC, Australia; [35]Department of Paediatrics, University of Melbourne, Parkville, VIC 3052, Australia; [36]Genetics Laboratory, Parc Taulí Hospital Universitari, Institut d'Investigació i Innovació Parc Taulí I3PT, Universitat Autònoma de Barcelona, 08208 Sabadell, Spain; [37]Unitat de Genètica Clínica, Servei de Medicina Pediàtrica, Parc Taulí Hospital Universitari, Institut d'Investigació i Innovació Parc Taulí I3PT, Universitat Autònoma de Barcelona, 08208 Sabadell, Spain; [38]Department of Pediatrics, NYU Grossman School of Medicine, New York, NY, USA; [39]Department of Pediatrics, The First Affiliated Hospital, Guangxi Medical University, Nanning, Guangxi, China; [40]Wessex Clinical Genetics Service, University Hospital Southampton, Princess Anne Hospital, Southampton SO16 5YA, UK; [41]Human Development and Health, Faculty of Medicine, University of Southampton, Southampton, UK; [42]Wessex Regional Genetics Laboratory, Salisbury NSF Foundation Trust, Salisbury District Hospital, Salisbury, UK; [43]Newcastle University Translational and Clinical Research Institute, Newcastle upon Tyne, UK; [44]Great North Children's Hospital, Newcastle upon Tyne Hospitals NHS Foundation Trust, Newcastle upon Tyne, UK; [45]Newcastle Hospitals, Newcastle upon Tyne, UK; [46]The Newcastle upon Tyne Hospitals NHS Foundation Trust, Institute of Genetic Medicine, Newcastle upon Tyne, UK; [47]Department of Clinical Genetics, Medical University in Bialystok, Bialystok, Poland; [48]Hospices Civils de Lyon, Groupe Hospitalier Est, Service de génétique, Bron, France; [49]Université de Lyon, University Lyon 1, CNRS, INSERM, Physiopathologie et Génétique du Neurone et du Muscle, UMR5261, U1315, Institut NeuroMyoGène, Lyon, France; [50]Australian Genomics Health Alliance, Melbourne, VIC, Australia; [51]Department of Paediatrics, Melbourne Medical School, University of Melbourne, Melbourne, VIC, Australia; [52]Bruce Lefroy Centre for Genetic Health Research, Murdoch Children's Research Institute, Royal Children's Hospital, Parkville, VIC, Australia; [53]Institute of Medical Genetics and Applied Genomics, University of Tübingen, Tübingen, Germany; [54]Klinik für Neuropädiatrie und angeborene Stoffwechselerkrankungen, Klinikum Oldenburg, Oldenburg, Germany; [55]Center for Rare Childhood Disorders, Translational Genomics Research Institute, Phoenix, AZ 85004, USA; [56]Division of Genetics and Genomic Medicine, Department of Pediatrics, Washington University School of Medicine, One Children's Place, St. Louis, MO, USA; [57]Department of Pediatric Neurology, Washington University School of Medicine, St. Louis, MO, USA; [58]Centre for Rare Diseases, University of Tübingen, Tübingen, Germany; [59]Division of Pediatric Neurology and Metabolic Medicine, Department of Pediatrics I, Medical Faculty of Heidelberg, Heidelberg University, Heidelberg, Germany; [60]Neuroscience Unit, KEMRI-Wellcome Trust, Center for Geographic Medicine Research Coast, Kilifi, Kenya; [61]Department of Pediatrics, Erasmus MC University Medical Center, Rotterdam, the Netherlands; [62]ENCORE Expertise Center for Neurodevelopmental Disorders, Erasmus MC University Medical Center, Rotterdam, the Netherlands; [63]Department of Neurology and Pediatric Neurology, Erasmus MC University Medical Center, Rotterdam, the Netherlands; [64]Department of Clinical Genetics, Erasmus MC University Medical Center, Rotterdam, the Netherlands; [65]Discovery Unit, Department of Clinical Genetics, Erasmus MC University Medical Center, Rotterdam, the Netherlands; [66]Department of Clinical Genetics, Lavender House, Birmingham Women's and Children's Hospital NHS Foundation Trust, Birmingham, UK; [67]Hospitaux Universitaires Genève, Geneva, Switzerland; [68]Department of Pediatrics-Medical Genetics, Duke University School of Medicine, Durham, NC, USA; [69]Institute of Human Genetics, Klinikum rechts der Isar, Technical University of Munich, School of Medicine and Health, Munich, Germany
[70]Further details can be found in the supplemental information
[71]These authors contributed equally
*Correspondence: gunnar.douzgos.houge@helse-bergen.no (G.D.H.), veerle.janssens@kuleuven.be (V.J.)
https://doi.org/10.1016/j.ajhg.2025.01.021.

Please cite this article in press as: Verbinnen et al., Pathogenic *de novo* variants in *PPP2R5C* cause a neurodevelopmental disorder within the Houge-Janssens syndrome spectrum, The American Journal of Human Genetics (2025), https://doi.org/10.1016/j.ajhg.2025.01.021

uncertain. Thr126del affects a highly conserved acidic loop, present in all B56 subunits, which for B56δ was shown to be involved in C-subunit binding[1] and short linear motif (SLiM)-containing substrate binding,[15] and for B56β was proposed to affect binding of tyrosine hydroxylase, a PP2A-B56β substrate without a B56-interacting SLiM.[22] More recent cryo-electron microscopy data inferred that residues in this loop are part of a complicated, still poorly understood regulatory network that involves very dynamic interactions between several domains of the B56δ subunit and the catalytic site of the C subunit.[23]

Similarly to *PPP2R5D*, *PPP2R5C* is ubiquitously expressed in many tissues.[24,25] At the cellular level, B56γ and B56δ proteins are present in the cytoplasm and the nucleus of most cell types.[24,26] While *in vivo* studies in *Ppp2r5d* knockout (KO) mice clearly revealed neuronal phenotypes,[27–29] *Ppp2r5c* KO mice suffer from heart problems (septal defects) and obesity.[30] Liver-specific *Ppp2r5c* KO mice showed increased lipogenesis and glucose uptake by impaired regulation of AMPK signaling and SRBP1 dephosphorylation.[31] Interestingly, double *Ppp2r5c*/*Ppp2r5d* KO mice are not viable and die around embryonic day 12 (E12),[32] further demonstrating the essential functions of both genes and suggesting an evolutionary overlap.[33] Notably, as for B56δ,[34,35] B56γ subunits confer major tumor-suppressive functions to PP2A in diverse cell models,[36,37] supposedly by their ability to dephosphorylate the oncogenic kinase AKT[38] and some of its substrates, including p27/KIP.[39] In other contexts, PP2A-B56γ holoenzymes dephosphorylate the mitogen-activated protein kinase (MAPK) ERK[40] and the mTOR substrate p70-S6 kinase,[41,42] further establishing their anti-proliferative properties. Other described cellular B56γ substrates include paxillin,[43] p53,[44,45] IκB kinase IKK,[46] and the mitotic regulators, BubR1 and Sgo2.[47,48]

Here, we report on 26 previously unpublished individuals with pathogenic or likely pathogenic *PPP2R5C* variants and describe the related clinical presentation. We identified 19 pathogenic *PPP2R5C* variants, five of which were recurrent and eight of which affect amino acids at orthologous positions of variants reported for *PPP2R5D* (6/8 showing the same missense variation). We have also collected individuals with *de novo* or inherited nonsense and consensus splice variants, all predicted to result in complete loss of function, and one individual with a familial complete gene deletion. We did not find clear evidence for such variants being pathogenic, i.e., for *PPP2R5C* haploinsufficiency. Biochemical characterization of these variants and of the single previously reported PPP2R5C variant Thr126del[2] revealed variable degrees of A/C subunit and substrate (liprin-α1) binding deficiencies and impaired catalytic activity, without clear correlation with clinical severity. Overall, our data establish *PPP2R5C* as another PP2A gene causally involved in neurodevelopmental disorders, further expanding the spectrum of HJS.

Subjects, material, and methods

Ethics statement

This study was performed according to the Declaration of Helsinki. All participants were ascertained by clinical diagnostics procedures, and parents gave clinical informed consent for testing. Their permission for inclusion in this collection of individuals with *PPP2R5C* variants, including photographs, was obtained using standard consent forms that were used and stored locally at each site. If required, each site was responsible for obtaining ethics approval for data sharing.

Cohort collection

We used a genotype-first approach through the GeneMatcher (GM) data-sharing platform[49] and data mining of aggregated DNA sequences from individuals with ultra-rare disorders across multiple research and diagnostic laboratories worldwide. Individuals with pathogenic *PPP2R5C* variants and complete clinical and phenotypic data were included. All 26 recently identified affected individuals were assessed by consultants in clinical genetics. Clinical and imaging data of affected individuals were collected using an extensive spreadsheet (Table S1).

Computational facial analysis

We applied the GestaltMatcher approach[50,51] to analyze facial similarities among ten subjects (P1, P5, P6, P7, P8, P21, P22, P23, P25, and P30; Figure 1, subject numbers in italics in Table 1) who consented to facial analysis within the *PPP2R5C* cohort; for details, see supplemental methods. These subjects were compared to a total of 1,555 images from various subjects with 328 different syndromes, which were selected from the GestaltMatcher Database (GMDB).[52] Two control distributions were then sampled: (1) distances between subjects sharing the same syndrome and (2) distances between random individuals with other disorders. Finally, the mean pairwise distance between individuals in the given cohort C was compared to these two distributions (Figure S1). In the end, we performed the pairwise comparison analysis on 11 images from individuals with *PPP2R5C* variants. To simulate the real-world scenario, we first compared 11 images from individuals with *PPP2R5C* variants to 7,459 images with 449 different disorders from GMDB. We performed leave-one-out cross-validation by putting the remaining images from ten individuals with *PPP2R5C* variants into the space with 7,459 images and calculating the ranks of ten *PPP2R5C* to the testing *PPP2R5C* individuals (Figure S2).

Generative adversarial network to synthesize participant portraits

To visualize the facial features associated with PPP2R5C we employed GestaltGAN,[53] a generative adversarial network (GAN) trained on 20 disorders that induce facial dysmorphism. During the training, our GAN learns to replicate

Figure 1. Facial photographs of ten individuals with *de novo PPP2R5C* missense variants
Numbers of individuals and variants are as indicated in Table 1. Framed pictures are from the same individual, and in three individuals from different time points. P6: (I) and (J) are from age 20 months, (K) from age 7 years; P30: (L) is from age 7 years, (M) and (N) from age 14 years; P25: (O) is from age 8 years, and (P) and (Q) from age 14 years.

Table 1. ***PPP2R5C*** **variants and associated phenotypic features**

	cDNA variant (NM_001352913.2)	Amino acid change (NP_848702.1)	dn	Individual #	Sex (M/F)	Age (y/mo)	NDD	Epil	H (*Z*)	OFC (*Z*)	Neonatal concerns	Hypotonia	Congenital malformation	Facial dysmorphism	ASD	Eye vision	Brain MRI
1	c.310T>C	p.Cys49Arg	Y	P36	F	16	+	+	N	+2.6	–	no	–	–	no	nystagmus	N
2	c.326_331del	p.Asp54_Phe55del	Y	P9	M	2/8	+	++	N	+2.2	–	no	–	no	no	N	N
3	c.330T>A	p.Phe55Leu	Y	P32	M	7	++	+++	+2	+5.4	–	yes	–	no	yes	N	large cisterna magna
4	c.524C>G	p.Pro120Arg	Y	*P21*	M	29	(+)	no	N	+5.2	–	mild	–	tall forehead, hypertelorism	no	N	N
5	c.529G>A	p.Glu122Lys	Y	*P1*	M	2/2	+++	++		N	–	yes	–	epicanthus	no	N	N
6	c.529G>A	p.Glu122Lys	Y	*P6*	M	1/8	+++	no	N	+3.6	jaundice	yes	–	tall forehead, hypertelorism	no	N	hyperintense white matter foci
7	c.529G>A	p.Glu122Lys	Y	*P8*	M	11	+++	++	−2.7	+4.8	–	yes	–	tall forehead	yes	N	hyperintense white matter foci
8	c.529G>A	p.Glu122Lys	Y	*P5*	F	10	+++	++	N	+3.2	–	yes	–	tall forehead, hypertelorism	yes	N	N
9	c.535G>A	p.Glu124Lys	Y	P35	F	5	+	no	N	+4	–	mild	–	–	no	N	–
10	c.540_542del	p.Thr126del	Y	P2	M	9	++	+	N	+3.3	poor feeding	–	–	telecanthus, high palate	–	N	–
11	c.552_554del	p.Ala130del	Y	P18	M	3	+++	++	−2	+2.2	poor feeding	yes	–	–	no	strabismus	mildly enlarged ventricles
12	c.552_554del	p.Ala130del	Y	P19	F	17	+++	+++	N	+6	poor feeding	yes	–	no	no	strabismus	N
13	c.556T>C	p.Trp131Arg	Y	P11	M	14	+++	+++	N	+4.4	lethargy	no	–	no	yes	N	abnormal sulcation
14	c.556T>C	p.Trp131Arg	?	P29	M	9	++	+++	N	+3	jaundice	no	–	no	no	N	–
15	c.563A>G	p.His133Arg	Y	P12	M	4/2	+(+)	no	N	+2.6	–	mild	–	tall forehead	no	N	slight CC hypoplasia
16	c.563A>G	p.His133Arg	Y	*P7*	M	10	+++	++	N	N	poor feeding, jaundice	mild	–	tall forehead	yes	CVI	hyperintense white matter foci
17	c.563A>C	p.His133Pro	Y	P26	F	16	+++	+++	N	N	poor feeding	yes	pyloric stenosis	tall forehead, high palate	–	CVI	mildly enlarged ventricles
18	c.563A>C	p.His133Pro	Y	P16	F	10	+	+++	N	N	poor feeding	mild	–	tall forehead, high palate	no	N	hippocampal sclerosis
19	c.563A>T	p.His133Leu	Y	P28	F	6	+	no	N	+2	poor feeding	mild	–	no	no	N	N
20	c.566T>C	p.Leu134Pro	Y	P10	M	2/4	+	no	N	+2.4	–	mild	coloboma	no	no	coloboma	large CC

(*Continued on next page*)

Please cite this article in press as: Verbinnen et al., Pathogenic *de novo* variants in *PPP2R5C* cause a neurodevelopmental disorder within the Houge-Janssens syndrome spectrum, The American Journal of Human Genetics (2025), https://doi.org/10.1016/j.ajhg.2025.01.021

Table 1. *Continued*

	cDNA variant (NM_001352913.2)	Amino acid change (NP_848702.1)	dn	Individual #	Sex (M/F)	Age (y/mo)	NDD	Epil	H (Z)	OFC (Z)	Neonatal concerns	Hypotonia	Congenital malformation	Facial dysmorphism	ASD	Eye vision	Brain MRI
21	c.685G>A	p.Glu174Lys	Y	*P30*	M	14	+	no	N	+3	nystagmus	mild	–	tall forehead	no	nystagmus, bilateral ptosis	large CC
22	c.689A>T	p.Asp175Val	Y	P14	F	2/6	+	++	N	+2	–	yes	–	tall forehead	no		N
23	c.694C>T	p.Arg177Trp	Y	*P25*	M	14	+	no	N	N	–	mild	bilateral foot deformity	?	no	N	N
24	c.695G>T	p.Arg177Leu[a]	?	P37	F	7	+	no	N	N	–	no	no	?	no	N	–
25	c.895A>G	p.Lys244Glu	Y	*P22*	F	2	(+)	no	−2	−2.8	poor feeding	yes	–	epicanthus	no	N	–
26	c.915A>C	p.Leu305Phe	?	P3	M	?	(+)	no	N	N	suspected drug exposure *in utero*	yes	no	flat occiput	no	N	N
27	c.1195G>A	p.Glu344Lys	Y	*P23*	F	1/2	+	no	N	+4.9	–	yes	coloboma	?	no	nystagmus	N

The first column shows the *PPP2R5C* cDNA variants according to the MANE Select transcript (NM_001352913.2), which does not correspond to the predicted amino acid changes in column 2. The amino acid changes refer to the shorter B56γ1 isoform (NP_848702.1), corresponding to the NM_178587.2 transcript. This is the transcript used for biochemical testing, from which all PPP2R5C missense changes are named.
NDD, neurodevelopmental delay; Epil, epilepsy/seizures, estimated to be from mild +, via moderate ++, to severe +++; H, height in SD when $Z > \pm 2$ SDs; OFC, occipito-frontal head circumference in SD when $Z > \pm 2$ SDs; ASD, autism spectrum disorder; degree of NDD: Y, present (degree unknown), (+) learning difficulties, + mild NDD, +(+) possibly moderate NDD, ++ moderate NDD, +++ severe NDD; dn, *de novo*; Y, yes; M, male; F, female; N, normal (also N if length or head circumference are within ± 2 SDs); –, no data. Individual numbers in italics indicate that facial images of these individuals were used for computational facial analysis.
[a]Individual added during the revision of the manuscript and not included in phenotype statistics, since this variant has not been biochemically tested.

the features associated with each syndrome within a latent space. Each disorder occupies a distinct region within this latent space, encapsulating its characteristic features. To obtain the latent representation for individuals with *PPP2R5C* variants, we utilized GAN inversion to locate the affected individuals within the latent space. The resulting features are then averaged and used to generate a portrait showcasing the characteristic features of the disorder (Figure 2).

Genetic testing and reporting of sequence variants

PPP2R5C sequence variants were collected as described above. Most variants were detected after routine diagnostic whole-exome sequencing.

Variant notation

In Table 1, all cDNA variants are annotated according to the MANE Select transcript of *PPP2R5C* (GenBank: NM_001352913.2), as now recommended for variant reporting. Since this transcript does not correspond to the shorter B56 isoform traditionally used for biochemical testing of *PPP2R5C* variants, we have not listed the corresponding protein change (p.) predicted by GenBank: NM_001352913.2 (MANE Select) cDNA change in Table 1 or in the remainder of the paper. This is to avoid confusion, since it is only from the shorter *PPP2R5C* isoform 1 transcript (GenBank: NM_178587.2, corresponding to GenBank: NP_848702.1 in Table 1, column 2) that all missense variants are known by the PP2A community, e.g., biochemists and cancer researchers, as well as healthcare operatives treating patients with HJS. This shorter transcript is also the transcript used by gnomAD for missense variant annotation. All (predicted) protein variants listed below therefore refer to the isoform 1 transcript NM_178587.2. In Table S1, the corresponding protein changes of the MANE Select transcript cDNA variants have been included for comparison (4th row).

In the results section, all protein variants are listed in p. nomenclature, in line with the rules for reporting DNA sequence-predicted protein changes. Because of the high number of missense variants, cDNA changes are not included in the text, but these can be found in Table 1. In the introduction and discussion, protein variants are written without the p., since this is no longer about reporting results but a discussion about variants' biochemical and medical consequences, and p. nomenclature is no longer relevant in such a setting.

Generation of *PPP2R5C* variants for biochemical testing

The coding region of the human B56γ isoform 1 (GenBank: NM_178587.2, corresponding to GenBank: NP_848702.1) was cloned into *Bam*HI-digested pEGFP-C1 vector using In-Fusion technology (Clontech). This plasmid was subsequently used as template for PCR-based site-directed mutagenesis (Stratagene) with proofreading Pwo DNA polymerase (Roche Applied Science) and complementary DNA oligonucleotides containing the desired

Figure 2. The representative face of ten *PPP2R5C* subjects generated by GAN inversion

point mutations (IDT, Table S2). All variants were confirmed by sequencing (LGC Genomics). Numbering of the variants is therefore according to B56γ isoform 1 (the full sequence of which is provided in Figure S3).

Cellular PP2A binding assays

HEK293T cells (ATCC, characterized by short tandem repeat profiling and mycoplasma-free) were transfected with PEI or PEIMAX transfection reagent using standard protocols. Forty-eight to 72 h post transfection, cells were rinsed with PBS, lysed in 150 μL of NET buffer (50 mM Tris-HCl [pH 7.4], 150 mM NaCl, 15 mM EDTA, and 1% Nonidet P-40) containing protease and phosphatase inhibitor cocktail (Roche Applied Science) and centrifuged for 15 min at 13,000 × *g*. If the experiment required measurement of phosphatase activity, Tris-buffered saline (TBS) was used instead of PBS, and phosphatase inhibitors were omitted from the lysis buffer.

For GFP pull-down experiments, lysates were incubated at 4°C for 1 h with 700 μL of NENT100 buffer (20 mM Tris-HCl [pH 7.4], 1 mM EDTA, 0.1% Nonidet P-40, 25% glycerol, and 100 mM NaCl) containing 1 mg/mL bovine serum albumin and 30 μL of GFP-trap-A beads (ChromoTek). Beads were washed three times with 1 mL of NENT300 (containing 300 mM NaCl), and two times with 1 mL of NENT150 (containing 150 mM NaCl). Bound proteins were eluted in 2× NuPage sample buffer (Invitrogen) and boiled for subsequent analysis by SDS-PAGE on 4%–12% (w/v) bis-Tris gels (Thermo Fisher Scientific) and western blotting. Membranes were blocked in 5% milk in TBS/0.1% Tween 20 for 1 h at room temperature and incubated with the primary antibody overnight at 4°C. Primary antibodies were mouse anti-GFP (B-2) (sc-9996), mouse anti-PP2A-A subunit (clone C5.3D10, generously supplied by Dr. S. Dilworth, Middlesex University, London, UK), mouse anti-PP2A-C subunit (clone F2.6A10, generously supplied by Dr. S. Dilworth, Middlesex University, London, UK), and rabbit anti-liprin-α1 (ProteinTech). After washing in TBS/0.1% Tween 20, membranes were incubated with horseradish peroxidase-conjugated secondary antibodies (Dako for anti-mouse and Cell Signaling for anti-rabbit) and developed using Western Bright ECL (Advansta) on the ImageQuant LAS4000 scanner (GE Healthcare). All densitometric quantifications were carried out using Image Studio Lite software v.5.2.

PP2A activity assays

After GFP pull-down, beads were washed once more with 20 mM Tris-HCl (pH 8.0) and 1 mM DTT (Tris-DTT) and finally resuspended in 60 μL of Tris-DTT solution, of which 35 μL was diluted in 250 μL of Tris-DTT buffer. All assays were performed with 30 μL of this phosphatase suspension and 10 μL of 2 mM stock of different phosphopeptides for 10–20 min at 30°C (still in the linear range of the assay) (Table S3). The released free phosphate was determined by addition of BIOMOL Green (catalog no. BMLAK111-0250, Enzo). After 30 min of incubation at room temperature, absorbance at 620 nm was measured in a multi-channel spectrophotometer (Thermo Scientific). We obtained (mutant or WT) B56γ-associated phosphatase activity by correcting the measured absorbances to the input of GFP-tagged B56γ, as determined by immunoblotting with anti-GFP antibodies and quantification by Image Studio Lite software v.5.2. C-subunit-associated activity was calculated similarly by correcting the obtained absorbance values to the quantified coprecipitating C-subunit signals (immunoblotting with anti-C antibodies).

Statistics

Statistical analysis of biochemical data was conducted by a one-sample Student's t test with false discovery rate (FDR) correction for multiple testing, in which the data were compared with WT values that were set at 100% in each experimental (biological) replicate. p values of less than 0.05 were considered significant ($^{*}p \leq 0.05$, $^{**}p \leq 0.01$, $^{***}p \leq 0.001$, $^{****}p \leq 0.0001$).

Results

Mutational spectrum of *PPP2R5C*-affected individuals

We describe 19 *PPP2R5C* alterations in 26 individuals, and include functional characterization of the single previously reported PPP2R5C (NP_848702.1) variant p.Thr126del (Table 1 and Figure 3A). All variants below refer to NP_848702.1, corresponding to PPP2R5C isoform 1 and the NM_178587.2 transcript (see variant notation in the subjects, material, and methods section for an explanation). One recently added variant, p.Arg177Leu, has not been functionally characterized but is likely pathogenic, since another variant of the same position, p.Arg177Trp, clearly affects PPP2R5C function. The individual with this biochemically untested variant has not been included in the

Please cite this article in press as: Verbinnen et al., Pathogenic *de novo* variants in *PPP2R5C* cause a neurodevelopmental disorder within the Houge-Janssens syndrome spectrum, The American Journal of Human Genetics (2025), https://doi.org/10.1016/j.ajhg.2025.01.021

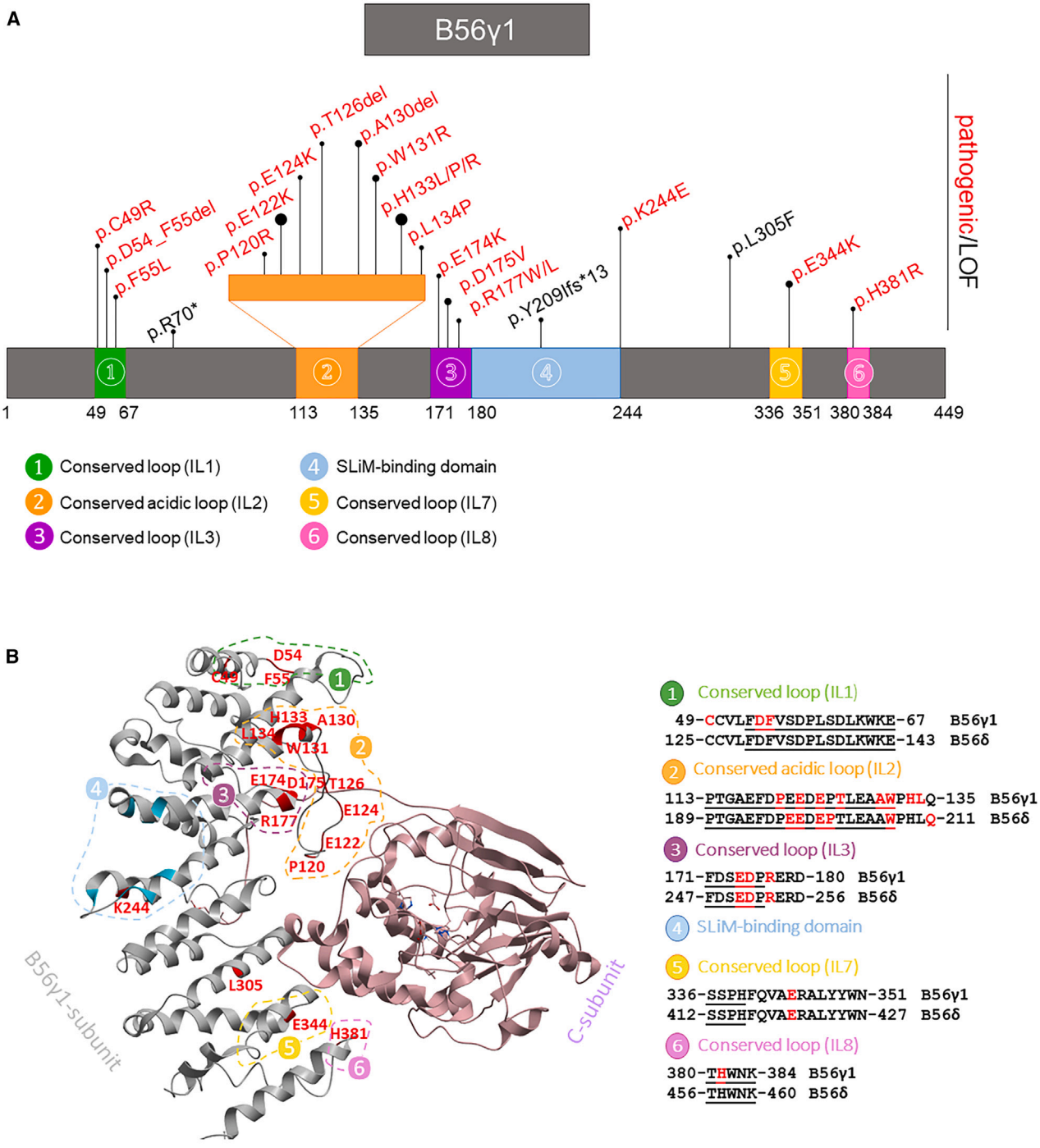

Figure 3. Missense variant hotspots in PPP2R5C

(A) Lollipop diagram showing the location of pathogenic (in red) and potentially pathogenic (loss-of-function) variants (in black) within B56γ1.

(B) Structural representation of the PPP2R5C variants reported in this study. Ribbon diagram of PP2A B56γ1 (in gray) and C subunit (in sepia) based on the published crystal structure of the PP2A B56γ1 holoenzyme by Cho and Xu (PDB: 2IAE)[54] were visualized in Molsoft MolBrowser v.3.9-2d software (ICM-Browser-Pro). Both B56γ1 and C lie on top of the horseshoe-shaped A subunit that was omitted from the structural representation to increase overall clarity. B56γ1 consists of 8 pseudo-HEAT repeats, with each pseudo-HEAT repeat harboring two anti-parallel α helices connected with an intra-repeat loop (IL). The large majority of pathogenic PPP2R5C variants affect amino acids residing in IL1, IL2 (acidic loop), IL3, IL7, and IL8 that are all facing the C subunit, and with the acidic loop (IL2) making direct contacts with the C subunit catalytic site. These intra-repeat loops are all highly conserved between B56γ and B56δ but are considerably differently affected in PPP2R5C- versus PPP2R5D-affected individuals (altered amino acids are highlighted in red; amino acids constituting the IL loops are underlined).

Please cite this article in press as: Verbinnen et al., Pathogenic *de novo* variants in *PPP2R5C* cause a neurodevelopmental disorder within the Houge-Janssens syndrome spectrum, The American Journal of Human Genetics (2025), https://doi.org/10.1016/j.ajhg.2025.01.021

phenotypic result statistics (see below). All individuals with known parental variant status (24/27) had *de novo* variants, resulting in missense variants (23 individuals) and in-frame deletions of 1–2 amino acids (four individuals) (Tables 1 and S4). One nonsense variant and one deletion of the whole gene were inherited, and one nonsense variant, one consensus splice site variant, and one frameshifting single-nucleotide deletion were *de novo* (Table S5). These loss-of-function variant individuals (biochemically confirmed for p.Arg70* and p.Tyr209Ilefs*13, Table S4) were not included among the 26 previously unreported individuals due to uncertain clinical relevance of the variants. Five *de novo* variants were recurrent: p.Glu122Lys (four individuals), p.Ala130del (two individuals), p.Trp131Arg (two individuals), p.His133Arg (two individuals), and p.His133Pro (two individuals). All described missense variants are absent from large population databases (gnomAD v.4.1) and affect highly conserved residues of B56γ (Figure 3 and Table S4). Alignment with *PPP2R5D* identified that eight *PPP2R5C* variants—p.Glu122Lys, p.Glu124Lys, p.Trp131Arg, p.Glu174Lys, p.Asp175Val, p.Arg177Trp, p.Arg177Leu, and p.Glu344Lys—occurred at orthologous positions, in six of eight instances having identical missense variation to known pathogenic *PPP2R5D* variants.[1,4,13–18]

The large majority of affected amino acids in B56γ reside in or near one of the intra-repeat loops (IL) of the eight described pseudo-HEAT repeats determined through crystallographic studies.[54,55] These loops all face the catalytic subunit (Figure 3B), with Glu122 in IL2 (the acidic loop) directly interacting with the catalytic subunit[54] and the corresponding residue in PP2A-B56β required for substrate dephosphorylation.[22] Eight affected PPP2R5C residues (Pro120, Glu122, Glu124, Thr126, Ala130, Trp131, His133, and Leu134) all localize to this acidic loop, which is also recurrently affected in HJS type 1 (*PPP2R5D*) (Figure 3B), albeit in a slightly different way. While the top residue in IL2 (Glu198 in B56δ; Glu122 in B56γ) is by far the most frequently altered in B56δ, His133 was assessed to be the most affected residue in B56γ (Figures 3A and S4). Moreover, some B56γ variants (Pro120, Thr126, Ala130, His133, and Leu134) have no reported pathogenic B56δ variants at orthologous positions in ClinVar or the literature, while, conversely, some pathogenic B56δ variants had no B56γ variants in orthologous positions (Glu197, Pro201, and Gln211, Figure S4A). Likewise, in the cohort of individuals with *PPP2R5C* variants reported in this study, the variants identified in IL1 (Cys49, Asp54, and Phe55) and IL8 (His381) have not been reported previously in individuals with *PPP2R5D*-related disorder (Figure S4B). The individual with the p.His381Arg variant has not been included in this cohort, due to lack of clinical information. Identical amino acids in B56γ and B56δ appear to be altered in IL3 (Glu174, Asp175, and Arg177) and IL7 (Glu344) (Figure S4C).

Two substituted amino acids do not reside in any of the B56 loops facing the C subunit: Lys244 is posed at the other side of the B56γ molecule, still within the SLiM-binding domain, a region shared by all B56 isoforms that serves to bind short LxxIxE motifs in B56-specific interactors or substrates[56]; and Leu305 is present within one of the α helices of pseudo-HEAT repeat 6 (Figure 3). Notably, none of the individuals with any of these two variants had phenotypes consistent with the HJS spectrum: the individual with p.Lys244Glu had transient hypotonia in infancy, short stature, and microcephaly; the individual with the p.Leu305Phe variant (unknown if *de novo*) had learning difficulties and no dysmorphic signs consistent with HJS.

PPP2R5C variants show functional defects in A-subunit, C-subunit, and/or substrate binding

To examine whether PP2A-B56γ holoenzyme formation and/or substrate binding were affected by the variants, WT B56γ and different B56γ variants were overexpressed as N-terminally GFP-tagged fusion proteins in human embryonic kidney (HEK293T) cells. First, their ability to interact with endogenous PP2A A and C subunits was assessed (Figure 4A). All observed binding effects were fully concordant for both A and C subunits, except for p.Pro120Arg and p.Lys244Glu with a C- but no A-binding defect (Figures 4B and 4C; Table S4). Relative to WT, A/C-binding defects were observed for 18 out of 20 missense/in-frame-deletion variants tested (Figures 4B and 4C; Table S4).

The potential changes in binding to liprin-α1, a reported B56γ interaction partner harboring a functional B56 LxxIxE-binding motif (SLiM), were also assessed (Figure 4A).[57,58] Liprin-α1 bound strongly to WT B56γ in our assays, and liprin-α1-binding defects were observed for 17 out of 20 of the B56γ variants tested (Figure 4D and Table S4).

In summary, 15 B56γ variants showed both a liprin-α1- and A/C-binding defect: p.Cys49Arg, p.Asp54_Phe55del, p.Phe55Leu, p.Glu122Lys, p.Thr126del, p.Ala130del, p.Trp131Arg, p.His133Arg, p.His133Pro, p.His133Leu, p.Leu134Pro, p.Glu174Lys, p.Asp175Val, p.Arg177Trp, and p.Leu305Phe (Figures 4A–4D and Table S4). Two variants, p.Glu124Lys and p.Glu344Lys, showed only a liprin-α1-binding defect; one variant, p.His381Arg, showed only an A/C-binding defect. Two variants, p.Pro120Arg and p.Lys244Glu, had unaffected liprin-α1 and A binding, but showed a C-binding defect (Figures 4A–4D and Table S4).

Some PPP2R5C variants are associated with reduced PP2A-B56γ-bound phosphatase activity

The intrinsic catalytic activity of the GFP-tagged PPP2R5C variants was determined on four different phospho-peptides, derived from three established PP2A-B56γ substrates (AKT phospho-Thr308, ERK phospho-Thr185, and p70 S6K phospho-Thr589) and one random, non-specific phospho-site (commercial peptide) using malachite green (Table S3). Results of activity assays were overall quite

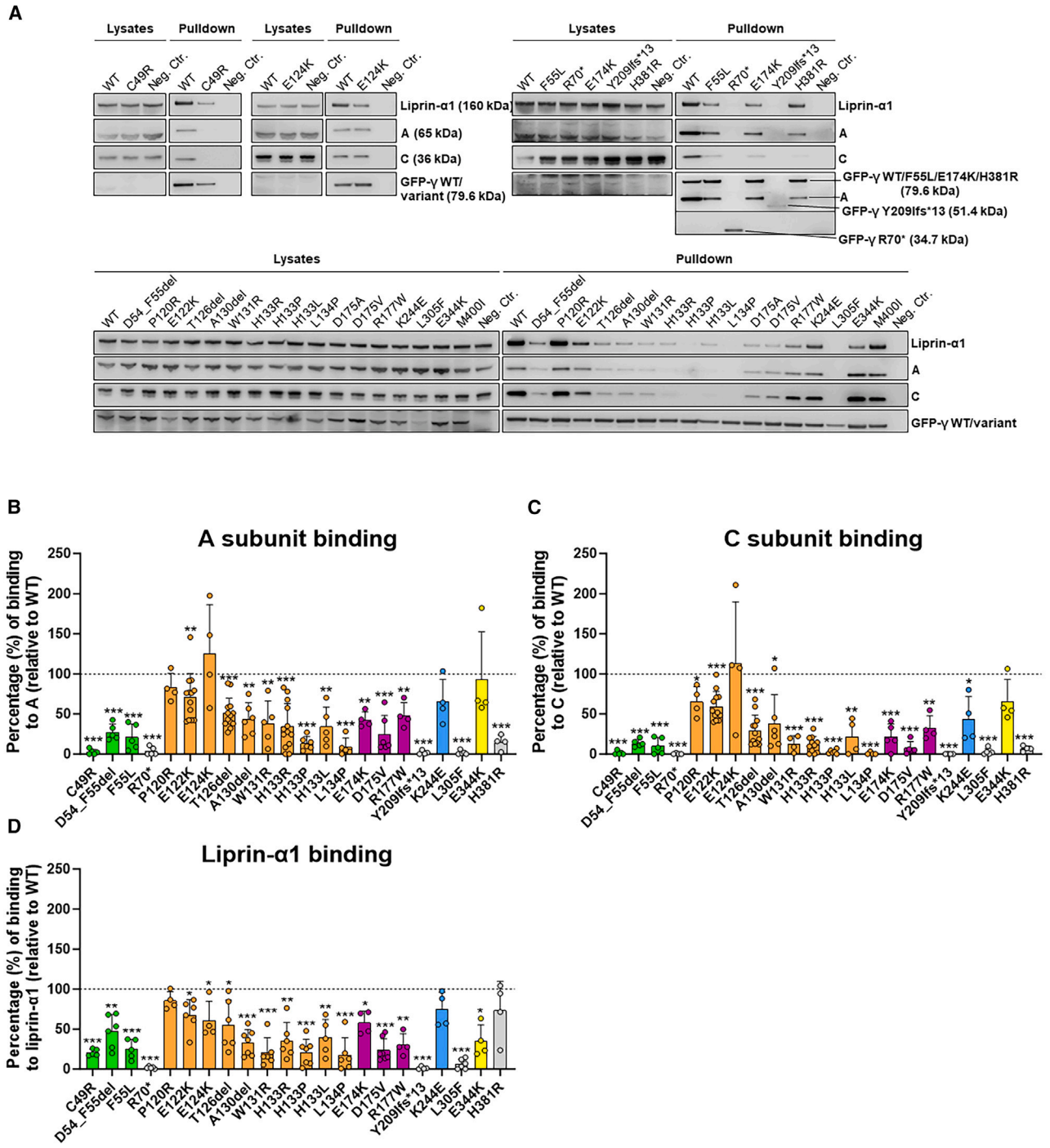

Figure 4. Functional characterization of *PPP2R5C* variants

(A) Representative immunoblots assessing binding of liprin-α1, PP2A A subunit, and PP2A C subunit to B56γ or its variants. GFP-tagged WT or variant B56γ subunits were purified from transfected HEK293T cells by GFP pull-down, and coprecipitation of endogenous PP2A-A, PP2A-C, and liprin-α1 was determined by immunoblotting (Neg. Ctr., GFP-only transfected condition).

(B–D) Quantification of binding abilities of GFP-tagged B56γ variants to the PP2A A subunit (B), C subunit (C), and the SLiM-containing PP2A substrate liprin-α1 (D). Immunoblot results were quantified and, for each individual variant, calculated relative to the immunoblot signals obtained for WT GFP-B56γ (present on the same blot and set at 100% in each independent experiment). Results represent the average values of at least four independent biological replicates ($n \geq 4$) ± SD. A one-sample t test with FDR correction for multiple testing (compared to 100%, i.e., WT value, dotted line) was used to determine statistical significance of the observed binding differences between each individual variant and WT (*$p \leq 0.05$, **$p \leq 0.01$, ***$p \leq 0.001$, ****$p \leq 0.0001$). The colors in these graphs correspond to the colors used to indicate the different loops and protein domains of B56γ in Figure 3.

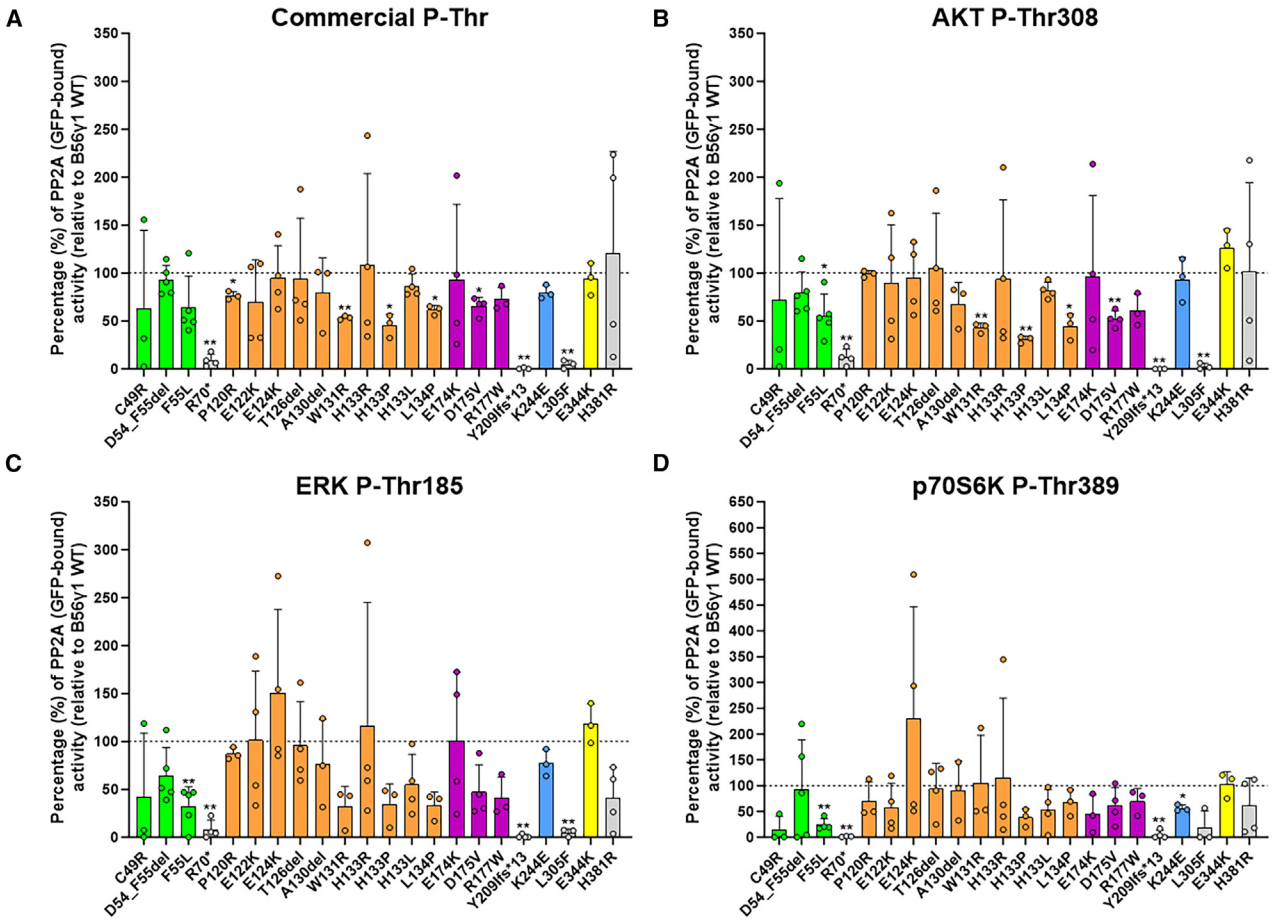

Figure 5. Phosphatase activity of *PPP2R5C* variants

Comparison of GFP-bound activities of *PPP2R5C* variants measured on a non-specific, commercial phospho-peptide (A) or on the indicated phospho-sites of established PP2A-B56γ substrates: AKT (B), ERK (C), and p70S6K (D) (phospho-peptide sequences: Table S3). PP2A activity was calculated relative to the GFP input of each variant (quantified by immunoblotting). The graphs represent the average PP2A activity ± SD for the *PPP2R5C* variants in comparison to activity of WT B56γ (set at 100% in each independent experiment, dotted line). Malachite green was used to quantify the released free phosphate. Results represent the average values of at least three independent biological replicates ($n \geq 3$) ± SD. A one-sample t test with FDR correction for multiple testing (compared to 100%, i.e., WT value) was used to determine statistical significance of the observed differences between each variant and the WT value of 100% (*$p \leq 0.05$, **$p \leq 0.01$, ***$p \leq 0.001$, ****$p \leq 0.0001$). The colors in these graphs correspond to the colors used to indicate the different loops and protein domains of B56γ in Figure 3.

consistent between these four phospho-peptide substrates (Figure 5 and Table S6). B56γ-specific activity was significantly decreased toward a canonical (commercial) phosphopeptide upon introduction of the p.Arg70*, p.Pro120Arg, p.Trp131Arg, p.His133Pro, p.Leu134Pro, p.Asp175Val, p.Arg177Trp, p.Tyr209Ilefs*13, and p.Leu305Phe variants (Figure 5A). Furthermore, phosphatase activity toward the AKT-P-Thr308 phosphopeptide was significantly decreased for the p.Phe55Leu, p.Arg70*, p.Trp131Arg, p.His133Pro, p.Leu134Pro, p.Asp175Val, p.Tyr209Ilefs*13, and p.Leu305Phe variants (Figure 5B). The p.Phe55Leu, p.Arg70*, p.Tyr209Ilefs13*, and p.Leu305Phe variants also showed decreased activity toward the ERK-P-Thr185 peptide (Figure 5C). Activity toward the P70S6K-P-Thr389 phosphopeptide was decreased for p.Phe55Leu, p.Arg70*, p.Tyr209Ilefs*13, and p.Lys244Glu (Figure 5D). While these differences in B56γ-normalized phosphatase activity likely largely reflect the differences in C-subunit binding to these variants (Figure 4C), we also normalized the assay data to the co-precipitating C subunit (which was quantified in all assay samples by anti-C immunoblotting). This logically results in increased specific activity of the associated C subunit on select phospho-peptides for a number of variants that show highly impaired C binding but a relatively smaller effect on GFP-bound activity (Figures S5A–S5D). An overview of all phosphatase assay data is given in Table S6. Of note, none of the B56γ proteins (neither WT nor variant) showed any phosphatase activity when a B55-specific phospho-peptide harboring a phospho-Ser-Pro site was used (Rb P-Thr252),[9] in accordance with published data.[59] Taken together, these data highlight that the PPP2R5C variants possibly affect major signaling pathways important for normal brain development and physiology by altering the phosphorylation state of the involved signaling kinases.

Clinical spectrum of *PPP2R5C*-affected individuals

We compiled a cohort of 26 *PPP2R5C*-affected individuals with complete clinical data, 11 females and 15 males who span an age range from 14 months to 29 years, and we have also included the previously reported single individual with the p.Thr126del in our overview (Table 1). The average age of the last examination by the clinician was 9 years. The *PPP2R5C*-related syndrome is a neurodevelopmental disorder characterized by stable developmental delay and intellectual disability of variable degrees (Figure 6A) and very frequent neonatal presentations ($>^3/_4$ of affected individuals) (Figures 6B and 6C). Among the most common reported features are generalized and sometimes persistent hypotonia (21/26), seizures (15/26), behavioral problems (13/24), and abnormal coordination (11/22) (Figures 6C–6E). The mean age of onset for seizures was 4.2 years; half of the individuals reported as seizure-free were younger, yet two were 14 and 29 years old, having p.Glu174Lys and p.Pro120Arg variants, respectively. The type of seizure is highly variable and includes recurrent status epilepticus (both with p.Ala130del, one with p.His133Pro, one with p.Trp131Arg, and one with p.Phe55Leu) and a combination of different seizure types, and sometimes the epilepsy is refractory to treatment (Figure 6E).

The majority (18/26) of affected individuals had large head circumference (>+2 standard deviations [SDs]) or macrocephaly, a term we only used on individuals with head circumferences >+2.5 SDs, since parental head circumferences were not available. Almost half (12/26) had a head circumference above +3 SDs (Table 1 and Figure 6B). There was a trend suggesting a positive correlation between macrocephaly and age for some of the recurrent variants (Figure 7) that needs confirmation in future studies, preferably by serial observations in the same individual.

Minor and sometimes unspecific brain MRI abnormalities of different types were reported in 9/22 individuals (Table 1). A range of behavioral problems was observed, including: difficulties in the regulation of emotions, fascination with light patterns, self-stimulation or self-harm, and repetitive behaviors such as chewing and teeth grinding for p.Asp54_Phe55del and p.Glu122Lys; restlessness and impulsiveness, need for routine and structure, aversion to loud noises, and sensory or attention deficit disorder for p.Cys49Arg, p.Arg177Trp, and p.Leu305Phe; and insomnia/sleep difficulties for p.Arg177Trp and p.Leu305Phe (Table S1 and Figure 6D).

The morbidity spectrum of the condition includes problems affecting the gastrointestinal (GI) system (8/25), sensory organs (10/23), and endocrine system (3/18). GI problems included frequent diarrhea for p.Glu122Lys, bloating intermittently and occasional constipation for p.Glu122Lys, bowel incontinence for p.Asp54_Phe55del, chronic and sometimes explosive diarrhea for p.Ala130del, and constipation for p.Arg177Trp and p.His133Pro. Sensory organ problems consisted of cerebral visual impairment for p.His133Arg and p.His133Pro, coloboma of the right eye for p.Leu134Pro, severe myopia and strabismus for p.Ala130del, and nystagmus for p.Cys49Arg and p.Glu344Lys. Endocrine problems were central precocious puberty for p.Glu122Lys and p.Ala130del, hypercalciuric hypercalcemia for p.Ala130del, hypercalciuria and nephrolithiasis for p.Arg177Trp, and type 2 diabetes for p.Ala130del. Some of the latter infrequent features are probably randomly associated with this subtype of HJS, but this remains to be seen.

Gestalt analysis

Affected individuals present a clinically overlapping gestalt characterized by dysmorphic features related to the macrocephaly (high and prominent forehead) but also arched eyebrows, hypertelorism, down-slanting palpebral fissures, low-set, retro-rotated external ears, low nasal bridge, and flared nostrils in the younger individuals and tendency to drooping cheeks in the older ones, as well as an almost constant round chin (Figure 1).

To create a standard visualization of the *PPP2R5C*-related craniofacial features, we employed GestaltGAN,[53] a GAN trained on 20 disorders that cause facial dysmorphism. During the training, the machine-learning model learns to replicate features characteristic to the disorder. To obtain the latent average for *PPP2R5C*-affected individuals, we perform GAN inversion to locate the affected individuals within the latent space. This process yields latent vectors containing the characteristic features specific to this disorder. By averaging these features and generating an image out of them, we create a portrait showcasing the characteristic features of the disorder (Figure 2). We also conducted facial dysmorphology analysis using GestaltMatcher to assess whether ten individuals with variants in *PPP2R5C* exhibited a similar facial phenotype. Initially, we examined the similarity at the cohort level. It was observed that 72% of the combinations of individuals with variants in *PPP2R5C* had a mean pairwise distance below the threshold ($c = 0.915$), indicating a significant similarity of facial phenotypes (Figure S1). Additionally, the pairwise comparison matrix revealed that six out of ten individuals had at least one match with a rank below 50, compared to 7,459 images encompassing 449 different disorders (Figure S2). Notably, only P21 and P22 did not exhibit significant similarity to the rest of the individuals with variants in *PPP2R5C*, the two individuals having variants with only a mild C-binding defect (Figure 4C). Conversely, P1, P5, and P6, sharing the same disease-causing variant, displayed remarkably high similarity. Hence, both results suggested that *PPP2R5C*-affected individuals share a similar facial gestalt.

Discussion

Dysfunction of PP2A or PPP2, a trimeric protein complex consisting of B (substrate binding), A (scaffolding), and C

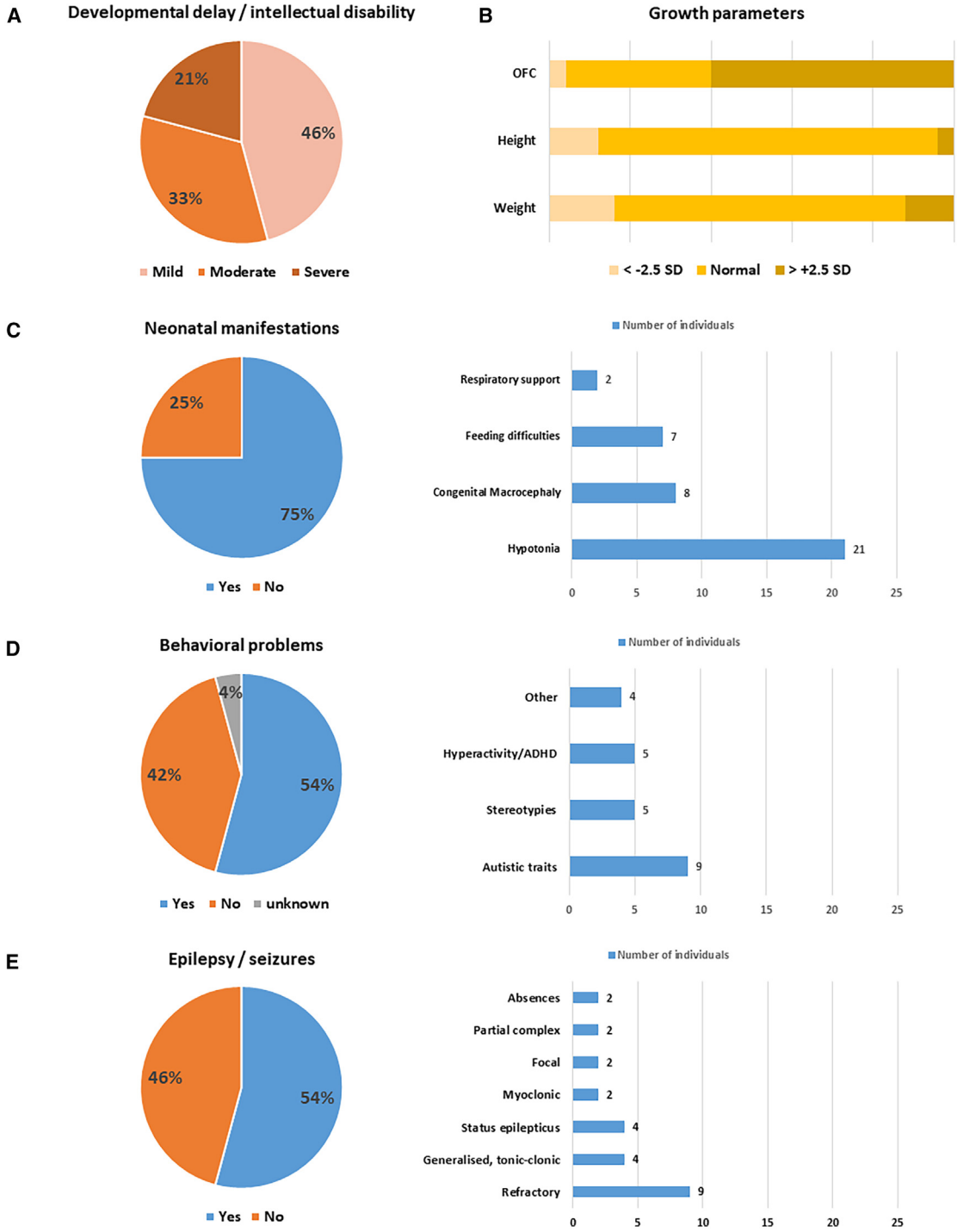

Figure 6. The clinical spectrum in the individuals with pathogenic *PPP2R5C* variants
About half of these individuals have mild intellectual disability/developmental delay; in the other half, the delay is moderate to severe (A). Growth parameters are within the normal range, except for an increased occipito-frontal head circumference (OFC) (B). Three-quarters of these individuals had neonatal concerns, such as feeding problems and hypotonia (C), and about half of them show behavior problems (D) or epilepsy (E).

(catalytic) subunits, has been correlated with neurodevelopmental delay after identifying pathogenic variants in *PPP2R5D*, encoding B56δ, *PPP2R1A*, encoding Aα, and *PPP2CA*, encoding Cα. Here, we summarize 27 individuals with *de novo* missense variants (23) or 1–2 amino acid deletions (4) in *PPP2R5C*, encoding another B-type subunit, B56γ, including the previously published individual with a *de novo* Thr126del variant (Table 1).[2] Five of these *de novo* variants were recurrent (Glu122Lys reported in four individuals, Ala130del reported in two individuals, Trp131Arg reported in two individuals, His133Arg reported in two individuals, and His133Pro reported in two

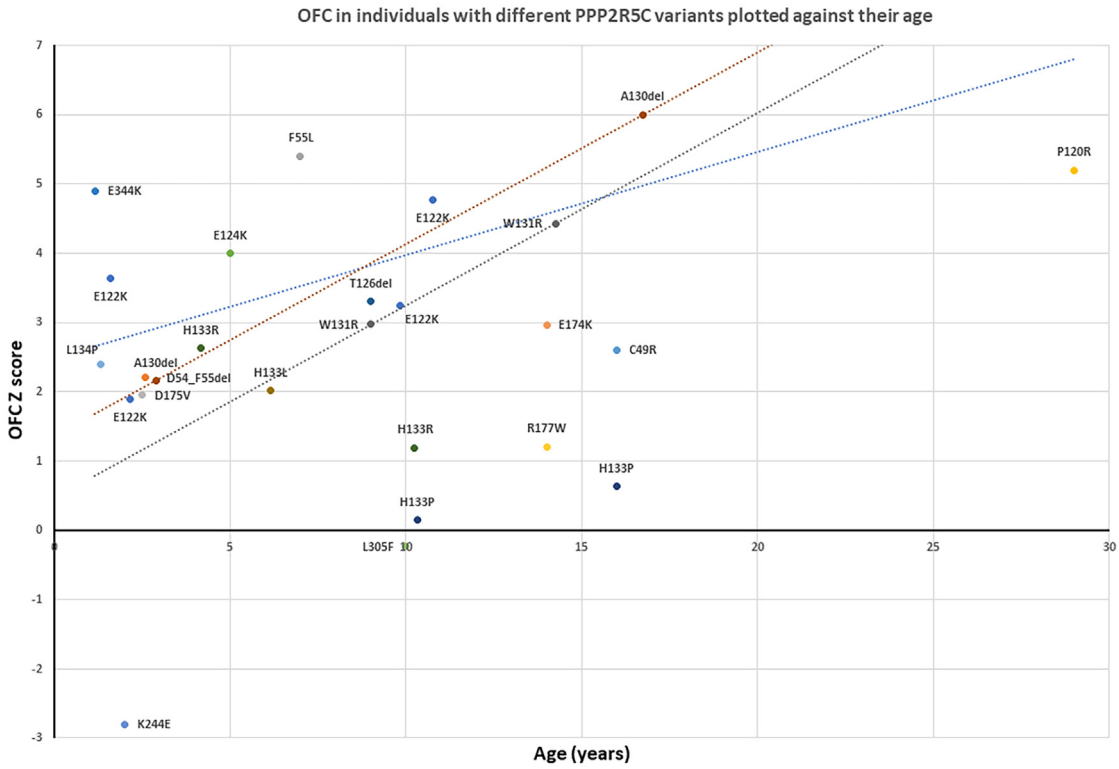

Figure 7. Head circumferences (OFCs) in the individuals with pathogenic *PPP2R5C* variants
Only one individual had microcephaly, while all the other head circumferences were from 0 to +6 SDs, and 14/26 OFCs were clearly in the macrocephalic range (>+2.5 SDs). For 3/5 variants with OFC observations at different ages (Glu122Lys, Ala130del, and Trp131Arg), there is a positive correlation with the age of the individuals, indicated by the three colored lines, one for each variant. The colors in this graph correspond to the colors used to indicate the different loops and protein domains of B56γ in Figure 3.

individuals), consistent with a beneficial effect on cell growth or survival at the time point of their occurrence. Of note, GeneDx recently published that they have found the Glu122Lys variant in five individuals, where at least two had phenotypes matching this cohort, and one of the variants was verified as *de novo*.[60]

In the three previously described genetic subtypes of syndromic PP2A dysfunction, there is a variable but overlapping range of phenotypic features, the most common being neurodevelopmental delay (from mild to severe intellectual disability), hypotonia, high risk of seizures, and dysmorphic features such as macrocephaly and frontal bossing in many. Recently, this has led to this clinical condition being named "Houge-Janssens syndrome" (HJS), and HJS is divided into type 1 caused by pathogenic *PPP2R5D* variants, type 2 caused by pathogenic *PPP2R1A* variants, and type 3 caused by pathogenic *PPP2CA* variants. In line with this, we suggest calling this novel subtype of HJS type 4, i.e., HJS4.

The phenotypic features of HJS4 are well within the range expected from the three other HJS subtypes (Table 1; Figures 6 and 7), but this additional subtype is more similar to HJS1 (*PPP2R5D*) than the two others. The main reason is a head circumference above average and in many individuals into the macrocephalic range (Figure 7), as well as dysmorphic features such as elongated face and frontal bossing (Figures 1 and 2). In HJS types 2 and 3, some individuals can even be microcephalic, but this is not a feature of HJS type 1 and the presented HJS subtype. One exception appears to be the individual with the Lys244Glu variant (P22) with a head circumference of −2.8 SDs and with a variant causing only mildly diminished C binding (Figure 4). Of note, the degree of intellectual disability appears, on average, to be milder in the presented subtype of HJS than in HJS type 1 due to a higher number of individuals with mild intellectual disability.

All included *PPP2R5C* variants except one (Arg177Leu) have been biochemically characterized with measurements of A/C binding and substrate binding, the latter to liprin-α1, or by measuring phosphatase activity toward small synthetic phospho-peptides containing known PP2A-B56γ dephosphorylation sites. Most variants (15) caused both liprin-α1- and A/C-binding defects, but two (Pro120Arg and Lys244Glu) had only a C-binding defect, and two (Glu124Lys and Glu344Lys) had only a liprin-α1-binding defect. There was no clear correlation between the nature or degree of these binding defects and clinical severity, but notably both variants with a C-binding defect only were associated with learning difficulties (Table 1). Mutant B56γ subunits with normal A/C binding but reduced substrate binding (such as Glu124Lys and Glu344Lys) could in theory cause a general reduction in

phosphatase activity by quenching A/C in inactive trimeric PP2A complexes (presuming that substrate binding is needed to activate the PP2A trimers), while mutant B56γ subunits with normal substrate but reduced C binding (like Pro120Arg and Lys244Glu) would exert a dominant-negative effect mainly on the substrate level and not on the general PP2A activity level. Interestingly, almost complete loss of A/C and liprin-α1 binding was seen in the 10-year-old boy with the Leu305Phe variant and a phenotype that appears to be in the learning difficulties but not intellectual disability range. It is not known whether the Leu305Phe variant is *de novo* or related to the individual's learning difficulties, but this individual is still included in Table 1. Mutant B56γ subunits that bind neither A/C nor substrates are deprived of exerting a dominant-negative effect on the substrate level (such as Glu344Lys), on the PP2A level (such as Pro120Arg and Lys244Glu), or on both levels (such as Leu305Phe). In addition, such free B subunits might be overall less stable.[61]

An area for further investigation would be to find the physiological substrates that have lost dephosphorylation dynamics due to retained B56γ binding but compromised A/C binding, i.e., a dominant-negative effect on the substrate level. The dominant-negative effect on the PP2A level due to inactive trimeric complexes is probably similar to C haploinsufficiency, another cause of mild intellectual disability.[3]

It should be properly understood that even though these B56γ variants are loss-of-function in a biochemical sense (lacking A/C binding and/or substrate binding), they are not loss-of-function in a genetic sense, since the main causative disease mechanism is likely to be dominant negative, i.e., a change of function. Although *PPP2R5C* has a gnomAD pLI of 1.00, there are too many predicted losses of function in the population to expect haploinsufficiency as a disease mechanism, at least for neurodevelopmental delay.[62] The gnomAD v.4.1 observed/expected loss-of-function ratio is 0.1, with 153 loss-of-function alleles of high technical quality. More importantly, the allele frequency of a 160-kb deletion removing almost the whole gene is 5% in NCBI dbVar (nssv16200169; 254/5,008 alleles), and the existence of this deletion polymorphism makes it highly unlikely that loss of one *PPP2R5C* allele has a negative phenotypic consequence. This also supports the hypothesis that the main pathogenic effect is on the substrate level through interference with phosphorylation-dephosphorylation dynamics, but with inactive trimeric PP2A complexes playing a contributory role.

Of additional note, two *de novo* pathogenic PPP2R5C variants identified in the current study (Cys49Arg and Glu174Lys) have previously been identified as somatic pathogenic mutants in persons with glandular tumor.[63,64] In line with our current findings, these variants exhibited major binding defects to the A/C core dimer, and, unlike WT B56γ, failed to suppress proliferation or anchorage-independent growth of HCT116 colon cancer cells, consistent with a loss of their tumor-suppressive function. Like B56δ, B56γ is indeed considered one of the major tumor-suppressive PP2A B-type subunits.[36,37,65]

In conclusion, we characterized 26 individuals with a neurodevelopmental delay that is most similar to HJS type 1 and that is caused by missense variants in *PPP2R5C* encoding B56γ. These amino acid changes affect PP2A holoenzyme formation and activity by reduced A/C binding and/or substrate binding, leading to reduced substrate dephosphorylation. The pathogenic effect is dominant negative, and individuals with nonsense, frameshifting, or whole-gene deletion variants do not appear to have abnormal phenotypes.

Data and code availability

The published article includes all datasets generated or analyzed during this study.

Acknowledgments

We are grateful to the participating families. We acknowledge Dr. A. Laenen (L-BioStat) for valuable advice on data analysis. This work has been generated within the European Reference Network on Rare Congenital Malformations and Rare Intellectual Disability (ERN-ITHACA; https://ern-ithaca.eu/) (EU Framework Partnership Agreement ID: 3HP-HP-FPA ERN-01-2016/739516). The Gestalt Matcher database (GMDB) is a service operated by the Association for Genome Diagnostics (AGD), which is a registered non-for-profit organization in Germany. GMDB aims to improve the openness and accessibility of scientific findings and to enhance collaboration among researchers and clinicians. GMDB is a non-profit community resource and is not linked to any one publisher or journal.

This work was generously funded by the Jordan's Guardian Angels Foundation and a research consortium fund from the State of California to V.J. and G.M. (sub-awards A19-3376-S005, A19-3376-S002, and A2853-S005). I.V. is a postdoctoral fellow of the Research Foundation Flanders and recipient of PDM funding obtained by the Internal Funds of KU Leuven. L.L. was co-funded by the Marguerite-Marie Delacroix Foundation. S.D.H. and G.D.H. are supported by a grant from the Norwegian National Advisory Unit on Rare Disorders (NKSD, project #43066). Other funder contributions can be found in the supplemental information.

Author contributions

Conceptualization, V.J. and G.D.H.; data curation, I.V. and S.D.H.; formal analysis, I.V., S.D.H., G.D.H., and V.J.; funding acquisition, I.V., V.J., S.D.H., T.S.B., E.O'H., E.G., S.M.W., T.B.H., and R.C.S.; investigation, all authors; methodology, V.J. and G.D.H.; project administration, V.J. and G.D.H.; software, T.-C.H. and H.L.; supervision, V.J. and G.D.H.; visualization, I.V., G.D.H., and S.D.H.; writing – original draft, I.V., S.D.H., V.J., and G.D.H.; writing – review and editing, all authors.

Declaration of interests

The authors declare no competing interests.

Web resources

gnomAD, https://gnomad.broadinstitute.org/
MANE Select, https://www.ncbi.nlm.nih.gov/refseq/MANE/
OMIM, https://omim.org/

Supplemental information

Supplemental information can be found online at https://doi.org/10.1016/j.ajhg.2025.01.021.

Received: August 27, 2024
Accepted: January 28, 2025
Published: February 19, 2025

References

1. Houge, G., Haesen, D., Vissers, L.E.L.M., Mehta, S., Parker, M.J., Wright, M., Vogt, J., McKee, S., Tolmie, J.L., Cordeiro, N., et al. (2015). B56δ-related protein phosphatase 2A dysfunction identified in patients with intellectual disability. J. Clin. Investig. *125*, 3051–3062. https://doi.org/10.1172/JCI79860.
2. Loveday, C., Tatton-Brown, K., Clarke, M., Westwood, I., Renwick, A., Ramsay, E., Nemeth, A., Campbell, J., Joss, S., Gardner, M., et al. (2015). Mutations in the PP2A regulatory subunit B family genes *PPP2R5B*, *PPP2R5C* and *PPP2R5D* cause human overgrowth. Hum. Mol. Genet. *24*, 4775–4779. https://doi.org/10.1093/hmg/ddv182.
3. Reynhout, S., Jansen, S., Haesen, D., van Belle, S., de Munnik, S.A., Bongers, E.M.H.F., Schieving, J.H., Marcelis, C., Amiel, J., Rio, M., et al. (2019). *De novo* mutations affecting the catalytic Calpha subunit of PP2A, *PPP2CA*, cause syndromic intellectual disability resembling other PP2A-related neurodevelopmental disorders. Am. J. Hum. Genet. *104*, 139–156. https://doi.org/10.1016/j.ajhg.2018.12.002.
4. Verbinnen, I., Vaneynde, P., Reynhout, S., Lenaerts, L., Derua, R., Houge, G., and Janssens, V. (2021). Protein Phosphatase 2A (PP2A) mutations in brain function, development, and neurologic disease. Biochem. Soc. Trans. *49*, 1567–1588. https://doi.org/10.1042/BST20201313.
5. Janssens, V., and Goris, J. (2001). Protein phosphatase 2A: a highly regulated family of serine/threonine phosphatases implicated in cell growth and signalling. Biochem. J. *353*, 417–439. https://doi.org/10.1042/0264-6021:3530417.
6. Lambrecht, C., Haesen, D., Sents, W., Ivanova, E., and Janssens, V. (2013). Structure, regulation, and pharmacological modulation of PP2A phosphatases. Methods Mol. Biol. *1053*, 283–305. https://doi.org/10.1007/978-1-62703-562-0_17.
7. Cheng, E., Cobben, J., and Ismayilova, N. (2022). A novel *PPP2CA* gene variant presenting with dystonia and progressive brain atrophy. J. Pediatr. Neurol. Neurosci. *6*, 202–206. https://doi.org/10.36959/595/439.
8. Verbinnen, I., Procknow, S.S., Lenaerts, L., Reynhout, S., Mehregan, A., Ulens, C., Janssens, V., and King, K.A. (2022). Clinical and molecular characteristics of a novel rare *de novo* variant in *PPP2CA* in a patient with a developmental disorder, autism, and epilepsy. Front. Cell Dev. Biol. *10*, 1059938. https://doi.org/10.3389/fcell.2022.1059938.
9. Lenaerts, L., Reynhout, S., Verbinnen, I., Laumonnier, F., Toutain, A., Bonnet-Brilhault, F., Hoorne, Y., Joss, S., Chassevent, A.K., Smith-Hicks, C., et al. (2021). The broad phenotypic spectrum of PPP2R1A-related neurodevelopmental disorders correlates with the degree of biochemical dysfunction. Genet. Med. *23*, 352–362. https://doi.org/10.1038/s41436-020-00981-2.
10. Douzgos, S., Janssens, V., and Houge, G. (2022). PPP2R1A-Related Neurodevelopmental Disorder. In GeneReviews® [Internet], M.P. Adam, H.H. Ardinger, R.A. Pagon, S.E. Wallace, L.J.H. Bean, G. Mirzaa, and A. Amemiya, eds. (University of Washington, Seattle), pp. 1993–2024.
11. Baker, E.K., Solivio, B., Pode-Shakked, B., Cross, L.A., Sullivan, B., Raas-Rothschild, A., Chorin, O., Barel, O., Bar-Yosef, O., Husami, A., et al. (2022). *PPP2R1A* neurodevelopmental disorder is associated with congenital heart defects. Am. J. Med. Genet. *188*, 3262–3277. https://doi.org/10.1002/ajmg.a.62946.
12. Qian, Y., Jiang, Y., Wang, J., Li, G., Wu, B., Zhou, Y., Xu, X., and Wang, H. (2023). Novel variants of *PPP2R1A* in catalytic subunit binding domain and genotype-phenotype analysis in neurodevelopmentally delayed patients. Genes *14*, 1750. https://doi.org/10.3390/genes14091750.
13. Shang, L., Henderson, L.B., Cho, M.T., Petrey, D.S., Fong, C.T., Haude, K.M., Shur, N., Lundberg, J., Hauser, N., Carmichael, J., et al. (2016). De novo missense variants in *PPP2R5D* are associated with intellectual disability, macrocephaly, hypotonia, and autism. Neurogenetics *17*, 43–49. https://doi.org/10.1007/s10048-015-0466-9.
14. Mirzaa, G., Foss, K., Nattakom, M., and Chung, W.K. (2019). PPP2R5D-Related Neurodevelopmental Disorder. In Gene Reviews® [Internet], M.P. Adam, H.H. Ardinger, R.A. Pagon, S.E. Wallace, L.J.H. Bean, G. Mirzaa, and A. Amemiya, eds. (University of Washington, Seattle), pp. 1993–2024.
15. Oyama, N., Vaneynde, P., Reynhout, S., Pao, E.M., Timms, A., Fan, X., Foss, K., Derua, R., Janssens, V., Chung, W., and Mirzaa, G.M. (2023). Clinical, neuroimaging and molecular characteristics of *PPP2R5D*-related neurodevelopmental disorders: an expanded series with functional characterisation and genotype-phenotype analysis. J. Med. Genet. *60*, 511–522. https://doi.org/10.1136/jmg-2022-108713.
16. Kim, C.Y., Wirth, T., Hubsch, C., Németh, A.H., Okur, V., Anheim, M., Drouot, N., Tranchant, C., Rudolf, G., Chelly, J., et al. (2020). Early-onset Parkinsonism is a manifestation of the *PPP2R5D* p.E200K mutation. Ann. Neurol. *88*, 1028–1033. https://doi.org/10.1002/ana.25863.
17. Walker, I.M., Riboldi, G.M., Drummond, P., Saade-Lemus, S., Martin-Saavedra, J.S., Frucht, S., Bardakjian, T.M., Gonzalez-Alegre, P., and Deik, A. (2021). *PPP2R5D* genetic mutations and early-onset Parkinsonism. Ann. Neurol. *89*, 194–195. https://doi.org/10.1002/ana.25943.
18. Hetzelt, K.L.M.L., Kerling, F., Kraus, C., Rauch, C., Thiel, C.T., Winterholler, M., Reis, A., and Zweier, C. (2021). Early-onset parkinsonism in *PPP2R5D*-related neurodevelopmental disorder. Eur. J. Med. Genet. *64*, 104123. https://doi.org/10.1016/j.ejmg.2020.104123.
19. Papke, C.M., Smolen, K.A., Swingle, M.R., Cressey, L., Heng, R.A., Toporsian, M., Deng, L., Hagen, J., Shen, Y., Chung, W.K., et al. (2021). A disorder-related variant (E420K) of a PP2A-regulatory subunit (PPP2R5D) causes constitutively active AKT-mTOR signaling and uncoordinated cell growth. J. Biol. Chem. *296*, 100313. https://doi.org/10.1016/j.jbc.2021.100313.
20. Smolen, K.A., Papke, C.M., Swingle, M.R., Musiyenko, A., Li, C., Salter, E.A., Camp, A.D., Honkanen, R.E., and Kettenbach, A.N. (2023). Quantitative proteomics and

phosphoproteomics of PP2A-PPP2R5D variants reveal deregulation of RPS6 phosphorylation via converging signaling cascades. J. Biol. Chem. *299*, 105154. https://doi.org/10.1016/j.jbc.2023.105154.

21. Haesen, D., Abbasi Asbagh, L., Derua, R., Hubert, A., Schrauwen, S., Hoorne, Y., Amant, F., Waelkens, E., Sablina, A., and Janssens, V. (2016). Recurrent *PPP2R1A* mutations in uterine cancer act through a dominant-negative mechanism to promote malignant cell growth. Cancer Res. *76*, 5719–5731. https://doi.org/10.1158/0008-5472.CAN-15-3342.
22. Saraf, A., Oberg, E.A., and Strack, S. (2010). Molecular determinants for PP2A substrate specificity: charged residues mediate dephosphorylation of tyrosine hydroxylase by the PP2A/B′ regulatory subunit. Biochemistry *49*, 986–995. https://doi.org/10.1021/bi902160t.
23. Wu, C.G., Balakrishnan, V.K., Merrill, R.A., Parihar, P.S., Konovolov, K., Chen, Y.C., Xu, Z., Wei, H., Sundaresan, R., Cui, Q., et al. (2024). B56δ long-disordered arms form a dynamic PP2A regulation interface coupled with global allostery and Jordan's syndrome mutations. Proc. Natl. Acad. Sci. USA *121*, e2310727120. https://doi.org/10.1073/pnas.2310727120.
24. McCright, B., Rivers, A.M., Audlin, S., and Virshup, D.M. (1996). The B56 family of protein phosphatase 2A (PP2A) regulatory subunits encodes differentiation-induced phosphoproteins that target PP2A to both nucleus and cytoplasm. J. Biol. Chem. *271*, 22081–22089. https://doi.org/10.1074/jbc.271.36.22081.
25. Martens, E., Stevens, I., Janssens, V., Vermeesch, J., Götz, J., Goris, J., and Van Hoof, C. (2004). Genomic organisation, chromosomal localisation tissue distribution and developmental regulation of the PR61/B′ regulatory subunits of protein phosphatase 2A in mice. J. Mol. Biol. *336*, 971–986. https://doi.org/10.1016/j.jmb.2003.12.047.
26. Lee, T.Y., Lai, T.Y., Lin, S.C., Wu, C.W., Ni, I.F., Yang, Y.S., Hung, L.Y., Law, B.K., and Chiang, C.W. (2010). The B56gamma3 regulatory subunit of protein phosphatase 2A (PP2A) regulates S phase-specific nuclear accumulation of PP2A and the G1 to S transition. J. Biol. Chem. *285*, 21567–21580. https://doi.org/10.1074/jbc.M109.094953.
27. Kapfhamer, D., Berger, K.H., Hopf, F.W., Seif, T., Kharazia, V., Bonci, A., and Heberlein, U. (2010). Protein Phosphatase 2a and glycogen synthase kinase 3 signaling modulate prepulse inhibition of the acoustic startle response by altering cortical M-Type potassium channel activity. J. Neurosci. *30*, 8830–8840. https://doi.org/10.1523/JNEUROSCI.1292-10.2010.
28. Louis, J.V., Martens, E., Borghgraef, P., Lambrecht, C., Sents, W., Longin, S., Zwaenepoel, K., Pijnenborg, R., Landrieu, I., Lippens, G., et al. (2011). Mice lacking phosphatase PP2A subunit PR61/B′delta (Ppp2r5d) develop spatially restricted tauopathy by deregulation of CDK5 and GSK3beta. Proc. Natl. Acad. Sci. USA *108*, 6957–6962. https://doi.org/10.1073/pnas.1018777108.
29. Tadmouri, A., Kiyonaka, S., Barbado, M., Rousset, M., Fablet, K., Sawamura, S., Bahembera, E., Pernet-Gallay, K., Arnoult, C., Miki, T., et al. (2012). Cacnb4 directly couples electrical activity to gene expression, a process defective in juvenile epilepsy. EMBO J. *31*, 3730–3744. https://doi.org/10.1038/emboj.2012.226.
30. Varadkar, P., Despres, D., Kraman, M., Lozier, J., Phadke, A., Nagaraju, K., and McCright, B. (2014). The protein phosphatase 2A B56γ regulatory subunit is required for heart development. Dev. Dyn. *243*, 778–790. https://doi.org/10.1002/dvdy.24111.
31. Cheng, Y.S., Seibert, O., Klöting, N., Dietrich, A., Straßburger, K., Fernández-Veledo, S., Vendrell, J.J., Zorzano, A., Blüher, M., Herzig, S., et al. (2015). PPP2R5C couples hepatic glucose and lipid homeostasis. PLoS Genet. *11*, e1005561. https://doi.org/10.1371/journal.pgen.1005561.
32. Dyson, J.J., Abbasi, F., Varadkar, P., and McCright, B. (2022). Growth arrest of PPP2R5C and PPP2R5D double knockout mice indicates a genetic interaction and conserved function for these PP2A B subunits. FASEB Bioadv. *4*, 273–282. https://doi.org/10.1096/fba.2021-00130.
33. Sommer, L.M., Cho, H., Choudhary, M., and Seeling, J.M. (2015). Evolutionary analysis of the B56 gene family of PP2A regulatory subunits. Int. J. Mol. Sci. *16*, 10134–10157. https://doi.org/10.3390/ijms160510134.
34. Lambrecht, C., Libbrecht, L., Sagaert, X., Pauwels, P., Hoorne, Y., Crowther, J., Louis, J.V., Sents, W., Sablina, A., and Janssens, V. (2018). Loss of protein phosphatase 2A regulatory subunit B56δ promotes spontaneous tumorigenesis in vivo. Oncogene *37*, 544–552. https://doi.org/10.1038/onc.2017.350.
35. Domènech Omella, J., Cortesi, E.E., Verbinnen, I., Remmerie, M., Wu, H., Cubero, F.J., Roskams, T., and Janssens, V. (2023). A novel mouse model of combined hepatocellular-cholangiocarcinoma induced by diethylnitrosamine and loss of *Ppp2r5d*. Cancers *15*, 4193. https://doi.org/10.3390/cancers15164193.
36. Chen, W., Possemato, R., Campbell, K.T., Plattner, C.A., Pallas, D.C., and Hahn, W.C. (2004). Identification of specific PP2A complexes involved in human cell transformation. Cancer Cell *5*, 127–136. https://doi.org/10.1016/s1535-6108(04)00026-1.
37. Sablina, A.A., Hector, M., Colpaert, N., and Hahn, W.C. (2010). Identification of PP2A complexes and pathways involved in cell transformation. Cancer Res. *70*, 10474–10484. https://doi.org/10.1158/0008-5472.CAN-10-2855.
38. Rocher, G., Letourneux, C., Lenormand, P., and Porteu, F. (2007). Inhibition of B56-containing protein phosphatase 2As by the early response gene IEX-1 leads to control of Akt activity. J. Biol. Chem. *282*, 5468–5477. https://doi.org/10.1074/jbc.M609712200.
39. Lai, T.Y., Yen, C.J., Tsai, H.W., Yang, Y.S., Hong, W.F., and Chiang, C.W. (2016). The B56γ3 regulatory subunit-containing protein phosphatase 2A outcompetes Akt to regulate p27KIP1 subcellular localization by selectively dephosphorylating phospho-Thr157 of p27KIP1. Oncotarget *7*, 4542–4558. https://doi.org/10.18632/oncotarget.6609.
40. Kawahara, E., Maenaka, S., Shimada, E., Nishimura, Y., and Sakurai, H. (2013). Dynamic regulation of extracellular signal-regulated kinase (ERK) by protein phosphatase 2A regulatory subunit B56γ1 in nuclei induces cell migration. PLoS One *8*, e63729.
41. Hahn, K., Miranda, M., Francis, V.A., Vendrell, J., Zorzano, A., and Teleman, A.A. (2010). PP2A regulatory subunit PP2A-B′ counteracts S6K phosphorylation. Cell Metab. *11*, 438–444. https://doi.org/10.1016/j.cmet.2010.03.015.
42. Hsiao, K.C., Ruan, S.Y., Chen, S.M., Lai, T.Y., Chan, R.H., Zhang, Y.M., Chu, C.A., Cheng, H.C., Tsai, H.W., Tu, Y.F., et al. (2023). The B56gamma3-containing protein phosphatase 2A attenuates p70S6K-mediated negative feedback loop to enhance AKT-facilitated epithelial-mesenchymal transition

in colorectal cancer. Cell Commun. Signal. *21*, 172. https://doi.org/10.1186/s12964-023-01182-5.

43. Ito, A., Kataoka, T.R., Watanabe, M., Nishiyama, K., Mazaki, Y., Sabe, H., Kitamura, Y., and Nojima, H. (2000). A truncated isoform of the PP2A B56 subunit promotes cell motility through paxillin phosphorylation. EMBO J. *19*, 562–571. https://doi.org/10.1093/emboj/19.4.562.
44. Li, H.H., Cai, X., Shouse, G.P., Piluso, L.G., and Liu, X. (2007). A specific PP2A regulatory subunit, B56gamma, mediates DNA damage-induced dephosphorylation of p53 at Thr55. EMBO J. *26*, 402–411. https://doi.org/10.1038/sj.emboj.7601519.
45. Shouse, G.P., Cai, X., and Liu, X. (2008). Serine 15 phosphorylation of p53 directs its interaction with B56gamma and the tumor suppressor activity of B56gamma-specific protein phosphatase 2A. Mol. Cell Biol. *28*, 448–456. https://doi.org/10.1128/MCB.00983-07.
46. Breuer, R., Becker, M.S., Brechmann, M., Mock, T., Arnold, R., and Krammer, P.H. (2014). The protein phosphatase 2A regulatory subunit B56γ mediates suppression of T cell receptor (TCR)-induced nuclear factor-κB (NF-κB) activity. J. Biol. Chem. *289*, 14996–15004. https://doi.org/10.1074/jbc.M113.533547.
47. Vallardi, G., Allan, L.A., Crozier, L., and Saurin, A.T. (2019). Division of labour between PP2A-B56 isoforms at the centromere and kinetochore. Elife *8*, e42619. https://doi.org/10.7554/eLife.42619.
48. Varadkar, P., Abbasi, F., Takeda, K., Dyson, J.J., and McCright, B. (2017). PP2A-B56gamma is required for an efficient spindle assembly checkpoint. Cell Cycle *16*, 1210–1219. https://doi.org/10.1080/15384101.2017.1325042.
49. Sobreira, N., Schiettecatte, F., Valle, D., and Hamosh, A. (2015). GeneMatcher: a matching tool for connecting investigators with an interest in the same gene. Hum. Mutat. *36*, 928–930. https://doi.org/10.1002/humu.22844.
50. Hsieh, T.C., Bar-Haim, A., Moosa, S., Ehmke, N., Gripp, K.W., Pantel, J.T., Danyel, M., Mensah, M.A., Horn, D., Rosnev, S., et al. (2022). GestaltMatcher facilitates rare disease matching using facial phenotype descriptors. Nat. Genet. *54*, 349–357. https://doi.org/10.1038/s41588-021-01010-x.
51. Hustinx, A., Hellmann, F., Sumer, O., Javanmardi, B., Andre, E., Krawitz, P., and Hsieh, T.C. (2023). Improving deep facial phenotyping for ultra-rare disorder verification using model ensembles. In 2023 IEEE/CVF Winter Conference on Applications of Computer Vision (WACV) (IEEE/CVF), pp. 5007–5017. https://doi.org/10.1109/WACV56688.2023.00499.
52. Lesmann, H., Hustinx, A., Moosa, S., Klinkhammer, H., Marchi, E., Caro, P., Abdelrazek, I.M., Pantel, J.T., Hagen, M.T., Thong, M.K., et al. (2024). GestaltMatcher Database - A global reference for the facial phenotypic variability of rare human diseases. Preprint at medRxiv. https://doi.org/10.1101/2023.06.06.23290887.
53. Kirchhoff, A., Hustinx, A., Javanmardi, B., Hsieh, T.C., Brand, F., Moosa, S., Schultz, T., Solomon, B.D., and Krawitz, P. (2024). GestaltGAN: Synthetic photorealistic portraits of individuals with rare genetic disorders. Preprint at medRxiv. https://doi.org/10.1101/2024.07.18.24308205.
54. Cho, U.S., and Xu, W. (2007). Crystal structure of a protein phosphatase 2A heterotrimeric holoenzyme. Nature *445*, 53–57. https://doi.org/10.1038/nature05351.
55. Magnusdottir, A., Stenmark, P., Flodin, S., Nyman, T., Kotenyova, T., Gräslund, S., Ogg, D., and Nordlund, P. (2009). The structure of the PP2A regulatory subunit B56 gamma: the remaining piece of the PP2A jigsaw puzzle. Proteins *74*, 212–221. https://doi.org/10.1002/prot.22150.
56. Hertz, E.P.T., Kruse, T., Davey, N.E., López-Méndez, B., Sigurðsson, J.O., Montoya, G., Olsen, J.V., and Nilsson, J. (2016). A conserved motif provides binding specificity to the PP2A-B56 phosphatase. Mol. Cell *63*, 686–695. https://doi.org/10.1016/j.molcel.2016.06.024.
57. Arroyo, J.D., Lee, G.M., and Hahn, W.C. (2008). Liprin alpha1 interacts with PP2A B56gamma. Cell Cycle *7*, 525–532. https://doi.org/10.4161/cc.7.4.5390.
58. Ripamonti, M., Lamarca, A., Davey, N.E., Tonoli, D., Surini, S., and de Curtis, I. (2022). A functional interaction between liprin-α1 and B56γ regulatory subunit of protein phosphatase 2A supports tumor cell motility. Commun. Biol. *5*, 1025. https://doi.org/10.1038/s42003-022-03989-3.
59. Kruse, T., Gnosa, S.P., Nasa, I., Garvanska, D.H., Hein, J.B., Nguyen, H., Samsøe-Petersen, J., Lopez-Mendez, B., Hertz, E.P.T., Schwarz, J., et al. (2020). Mechanisms of site-specific dephosphorylation and kinase opposition imposed by PP2A regulatory subunits. EMBO J. *39*, e103695. https://doi.org/10.15252/embj.2019103695.
60. Muir, A.M., Reich, A., Zou, F., Carere, D.A., Harasink, S.M., Tran, L., and McGivern, B. (2024). A recurrent variant in *PPP2R5C* identified in individuals with macrocephaly, intellectual disability, and seizures. HGG Adv. *6*, 100394. https://doi.org/10.1016/j.xhgg.2024.100394.
61. Sents, W., Ivanova, E., Lambrecht, C., Haesen, D., and Janssens, V. (2013). The biogenesis of active protein phosphatase 2A holoenzymes: a tightly regulated process creating phosphatase specificity. FEBS J. *280*, 644–661. https://doi.org/10.1111/j.1742-4658.2012.08579.x.
62. Chen, S., Francioli, L.C., Goodrich, J.K., Collins, R.L., Kanai, M., Wang, Q., Alföldi, J., Watts, N.A., Vittal, C., Gauthier, L.D., et al. (2024). A genomic mutational constraint map using variation in 76,156 human genomes. Nature *625*, 92–100. https://doi.org/10.1038/s41586-023-06045-0.
63. Nobumori, Y., Shouse, G.P., Fan, L., and Liu, X. (2012). HEAT Repeat 1 motif is required for B56γ-containing Protein Phosphatase 2A (B56γ-PP2A) holoenzyme assembly and tumor-suppressive function. J. Biol. Chem. *287*, 11030–11036. https://doi.org/10.1074/jbc.M111.334094.
64. Nobumori, Y., Shouse, G.P., Wu, Y., Lee, K.J., Shen, B., and Liu, X. (2013). B56γ tumor-associated mutations provide new mechanism for B56γ-PP2A tumor suppressor activity. Mol. Cancer Res. *1*, 995–1003. https://doi.org/10.1158/1541-7786.MCR-12-0633.
65. Meeusen, B., and Janssens, V. (2018). Tumor suppressive protein phosphatases in human cancer: Emerging targets for therapeutic intervention and tumor stratification. Int. J. Biochem. Cell Biol. *96*, 98–134. https://doi.org/10.1016/j.biocel.2017.10.002.